



# An experimental study of drainage network development by surface and subsurface flow in low-gradient landscapes

Brian G. Sockness<sup>1</sup>, Karen B. Gran<sup>1</sup>

<sup>1</sup>Department of Earth and Environmental Sciences, University of Minnesota Duluth, Duluth, MN, USA

5 Correspondence to: Karen B. Gran (kgran@d.umn.edu)

**Abstract.** How do channel networks develop in low-gradient, poorly-drained landscapes? Rivers form elaborate drainage networks with morphologies that express the unique environments in which they developed, yet we lack an understanding of what drives channel development in low-gradient landscapes like those left behind in the wake of continental glaciation. To better understand what controls the erosional processes allowing channel growth and integration of non-contributing areas (NCA) over time, we conducted a series of experiments in a small-scale drainage basin. By varying substrate and precipitation, we could vary the partitioning of flow between the surface and subsurface, impacting erosional processes. Channels developed by overland flow and seepage erosion to varying extents depending on substrate composition, rainfall rate, and drainage basin relief. Seepage-driven erosion was favored in substrates with higher infiltration rates, while overland flow was more dominant in experiments with high precipitation rates. Overland flow channels formed at the onset of experiments and expanded over a majority of the basin area, forming broad dendritic networks. Large surface water contributing areas supported numerous first-order channels, allowing for more rapid integration of NCA than through seepage erosion. When overland flow was the dominant process, channels integrated NCA at a similar, consistent rate under all experimental conditions. Seepage erosion began later in experiments after channels had incised enough for exfiltrating subsurface flow to initiate mass wasting of headwalls. Periodic mass wasting of channel heads caused them to assume an amphitheater-shaped morphology. Seepage allowed for channel heads to expand with smaller surface water contributing areas than overland flow channels, allowing for network expansion to continue even with low CA. Seepage-driven channel heads integrated NCA more slowly than channel heads dominated by overland flow, but average erosion rates in channels extending through seepage erosion were higher. The experimental results provide insight into drainage networks that formed in glacial sediment throughout areas affected by continental glaciation, and highlight the importance of subsurface hydrologic connections in integrating and expanding drainage networks over time in these landscapes.

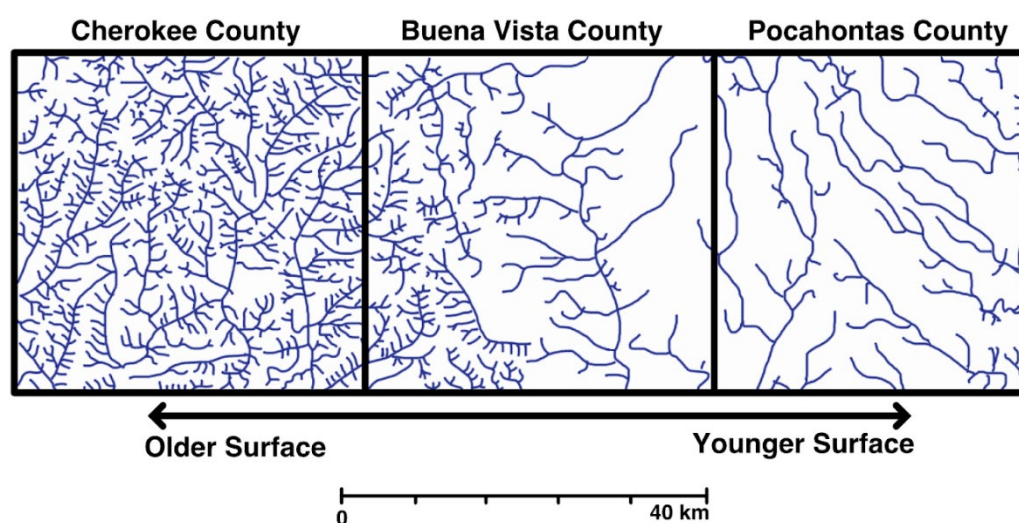
## 1 Introduction

Drainage networks form in settings with distinct geologic, climatic, and relief characteristics that largely control their development over long timescales (Schumm, 1981; Schumm and Lichty, 1965). Most research efforts exploring drainage network evolution have focused on networks in high-gradient settings (Altin and Altin, 2011; Babault et al., 2012; Castelltort



30 and Simpson, 2006; Daag, 2003; Daag and Van Westen, 1996; Garcia and Hérail, 2005; Hovius et al., 1998; Janda et al., 1984;  
 Maroukian et al., 2008; Simon, 1999; Winterberg and Willett, 2019). Low-gradient drainage networks are likely controlled by  
 similar factors, but fewer studies have investigated their long-term evolution. One barrier to drainage network development is  
 that rivers have to incorporate substantial amounts of internally-drained areas, referred to as non-contributing areas (NCAs),  
 into their watersheds to expand. The processes by which those NCAs are integrated into the drainage network may vary  
 35 between high-gradient and low-gradient upland settings.

Widespread, low-gradient uplands with abundant NCAs are common in regions impacted by continental glaciation. In the  
 Central Lowlands physiographic region of the United States, for example, multiple advances of the Laurentide Ice Sheet during  
 the Pleistocene scoured and deposited sediment across the region, reworking pre-existing river systems by damming, re-  
 routing, or filling in channels. Following glaciation, new drainage networks developed in the glacial deposits. In a classic  
 40 study, Ruhe (1952) observed the gradual reestablishment of drainage networks in Iowa, USA, where younger, more recently  
 glaciated surfaces had less extensive drainage networks than surfaces associated with earlier glaciations [Fig. 1]. Clearly  
 network development is occurring across these low-gradient uplands in Iowa and across the region over tens to thousands of  
 years, however we lack a process-based understanding of how integration proceeds in low-gradient landscapes with abundant  
 NCA.



45

**Figure 1. Drainage network development across three counties in northwestern Iowa, USA. Glacial deposits in Cherokee County were deposited during earlier glacial periods than deposits in Buena Vista and Pocahontas counties. Higher drainage densities occur on the older deposits compared to the younger deposits (modified from Ruhe, 1952).**



50 There are multiple ways by which rivers can capture NCA. One entails base level fall instigating headward erosion of channels as knickpoints propagate into the uplands: a bottom-up model of drainage network development. Headward erosion incorporates NCA into the drainage network by breaching the shallow drainage divides that isolate depressions. Studies conducted in low-gradient upland settings have found that base level fall can help initiate channel incision, generate relief, and perpetuate headward growth (Clayton and Moran, 1982; D'Alpaos et al., 2005, 2007; Fagherazzi et al., 2012; Gran et al., 2009, 55 2013; Matsch, 1983; Whipple et al., 2017). One of the limiting factors with bottom-up integration is that upstream area must be able to provide enough water at the channel tips to initiate erosion, a challenging condition in low-gradient terrains where substantial parts of upland areas are internally-drained.

A second method of network expansion takes more of a top-down approach, driven by connections of surface and subsurface water from NCAs to downstream channel heads, for example, by spillover of water contained in NCA depressions during 60 periods of sufficient precipitation. Spillover events can be transient, leading to dynamically-variable connectivity between NCA and downstream waters (Brooks et al., 2018; Leibowitz et al., 2016; Leibowitz and Vining, 2003; Rosenberry and Winter, 1997; Shaw et al., 2012; Stichling and Blackwell, 1957), or spillover events can incise a channel to create a permanent connection between NCA and the drainage network (Douglass et al., 2009; Douglass and Schmeckle, 2007; Hilgendorf et al., 2020). Hydrologic connections can also occur when groundwater flows from depressions to adjacent streams, driven by the 65 contrasting hydraulic conductivities of the region's glacial deposits (Labaugh et al., 1998; Neff and Rosenberry, 2018; Winter, 1999) or by regional groundwater flow patterns that allow subsurface flow to deviate from topographic divides and provide additional water to channels. If water contributed from NCA via the subsurface is able to erode channel tips through seepage erosion, then network integration can proceed via subsurface connections even in the absence of surface water connections.

The hydrologic subsidy provided by surface and subsurface connections between NCA and channels can have important 70 implications for the long-term development of drainage networks (Lai and Anders, 2018; Hilgendorf et al., 2020). If NCA are geographically isolated (Tiner, 2003) but not hydrologically isolated, then hydrologic contributions via the surface or subsurface can help integrate drainage networks. Numerical modeling by Lai and Anders (2018) showed that hydrologically-connected NCA are necessary to drive drainage network development in low-gradient landscapes. An important, unresolved issue is how water routed via the surface or subsurface to varying degrees drive different processes of channel development 75 and how that partitioning affects NCA integration. Geology, climate, vegetation, and relief differ throughout post-glacial landscapes of the Central Lowlands, which may favor surface or subsurface routing of potential NCA contributions. Deconvolving the impacts of these different variables is challenging in the field, particularly given recent anthropogenic impacts on these same post-glacial landscapes that have changed hydrologic connectivity (Foufoula-Georgiou et al., 2015; Schottler et al., 2014).

80 To better understand the processes that drive drainage integration via both surface and subsurface flow, we present the results from a series of drainage network evolution experiments. The experiments subjected an initially flat, internally-drained surface



to rainfall and continuous base level fall to incise channels through headward erosion. We tested different combinations of substrate composition and rainfall rates to investigate how these attributes mediate the partitioning of precipitation between the surface and subsurface, driving different processes of channel development. A terrestrial lidar scanner captured high-resolution topographic data of the developing drainage network to characterize channel development, the evolution of CA and NCA through time, and the rates and patterns of network growth. Our results show that overland flow and seepage erosion drove channel development to different extents based on experimental conditions that impacted infiltration capacity, rainfall delivery rate, and relief. The experiments provide insight into the processes by which drainage networks grow and highlight the importance of subsurface flow for drainage network growth in low-gradient landscapes.

## 2 Background

### 2.1 Processes of Channel Development

Water moving through and across landscapes forms channels by exerting sufficient force to entrain and erode sediment. Overland flow exerts shear stress on the surface as a function of slope and water depth. Erosion of channel heads that occurs due to concentration of flow and steeper slopes can lead to drainage-head erosion and network expansion. In addition, shallow subsurface or groundwater flow can create or grow channels when water emerges from the subsurface with enough force to cause seepage erosion (Dunne, 1990). Erosion via seepage is a function of hydraulic gradient and permeability of substrate. Larger hydraulic gradients increase seepage forces, which can occur if groundwater recharge is greater or the interface between the surface and subsurface has greater relief (Dunne, 1980, 1990). As channels expand by seepage erosion, groundwater flow further concentrates at the channel heads and begets more erosion by positive feedback (Dunne, 1990; Cullen and Anders, in review). Erosion at channel heads introduces asymmetries in the concentrated flow of groundwater, causing the direction of channel growth to adjust towards maintaining symmetrical flow (Cohen et al., 2015). The gradual erosion of sediment by seepage can eventually cause mass wasting by undermining the overlying material and eroding large volumes of sediment.

Seepage erosion has been studied at different spatial scales as a form of channel development. At large scales, seepage erosion has been attributed as the primary driver of channel development for drainage networks in unconsolidated materials (Coelho Netto et al., 1988; Micallef et al., 2021; Pillans, 1985; Schumm and Phillips, 1986; Uchupi and Oldale, 1994), and in bedrock in places like the Colorado Plateau (Howard, 1988; Laity and Malin, 1985) and Florida Panhandle (Schumm et al., 1995). The channel heads of these networks are often described as “amphitheater-shaped” due to the distinctive high relief headwalls that form when seepage erosion undermines channel headwalls and causes mass wasting (Laity and Malin, 1985), although this morphology may arise from any curvature-driven mechanical process (Petroff et al., 2018). Seepage erosion has also been linked to distinct longitudinal profiles (Devauchelle et al., 2011) and bifurcation angles (Petroff et al., 2013; Devauchelle et al., 2012), the latter being more prevalent in regions with humid climates favoring groundwater flow to streams (Seybold et



al., 2017, 2018). At smaller scales, seepage can drive gully erosion in relatively low-gradient agricultural settings (Castillo and Gómez, 2016).

115 The partitioning of flow to the surface vs. subsurface is largely a balance between water delivery to the surface by precipitation and water losses by infiltration into the subsurface. Determining this balance is complex because many factors controlling infiltration and evapotranspiration like vegetation type and density, substrate texture and saturation level, and topographic roughness are to some extent codependent on the precipitation rates and volumes set by the prevailing climate. Numerical models, physical experiments, and field-based studies are particularly useful approaches for determining the interactions and feedbacks between different subsets of these factors and their influence on infiltration and runoff generation (Dunne et al., 120 1991; Huang et al., 2013; Morbidelli et al., 2015; Mu et al., 2015; Nassif and Wilson, 1975; Thompson et al., 2010).

For this study, the effects of sediment texture and precipitation rates on infiltration and flow pathways in low-gradient upland settings are studied. In isolation, coarse-grained sediments have greater infiltration capacities than fine-grained sediments, allowing precipitation to infiltrate faster, potentially reducing the degree of surface water ponding. Also in isolation, greater rainfall rates provide larger volumes of water over a given timespan, increasing the likelihood of attaining saturation, surface 125 water ponding, and overland flow. However, the combined effects of slope, substrate texture, and rainfall rates on flow pathways remain difficult to determine, as reviewed by Morbidelli et al. (2015). They suggest that interactions between surface and subsurface water may be an important and largely unresolved factor controlling infiltration across different slopes, making it important to consider processes associated with both surface and subsurface water.

## 130 2.2 Previous Drainage Network Development Experiments

Physical experiments conducted in the laboratory allow us to study channel development under controlled conditions and reduced spatial scales. The apparatuses used to model channel development have typically incorporated three fundamental design elements: an erodible substrate, a precipitation source, and a mechanism to adjust base level. These elements simulate three of the major controls of drainage network development: geology, climate, and tectonics, respectively. Prior experiments 135 have investigated how changing these conditions affects the processes of drainage network development on an initially unchannelized surface (Bonnet and Crave, 2003; Hasbargen and Paola, 2000; Lague et al., 2003; Parker, 1977; Pelletier, 2003; Phillips and Schumm, 1987; Singh et al., 2015; Sweeney et al., 2015).

Parker (1977) showed that channel network development by overland flow followed the temporal phases of initiation, elongation, and elaboration first proposed by Glock (1931). Pelletier (2003) built on these results by testing channel network 140 growth under different topographic configurations. Similar to other studies (Phillips and Schumm, 1987), they found that



overland flow produced dendritic drainage networks at a rate dependent on the initial slope of a planar surface. However, convex plateau-like surfaces had a combination of channelization by both overland flow and seepage erosion.

Other experiments have shown how the development of drainage networks by overland flow can result in different steady-state topography under constant uplift and precipitation (Bonnet and Crave, 2003; Hasbargen and Paola, 2000; Lague et al., 2003). Lague et al. (2003) found that internally-drained areas were captured at an exponential rate before fully integrating the initial surface. Increasing the uplift rate caused the mean elevation to increase throughout the basin (Bonnet and Crave, 2003; Lague et al., 2003) and channel morphology adjusted to have a smaller cross-sectional area (Turowski et al., 2006). Ouchi (2011) described an episodic “erosion with knickpoints” mode of fluvial erosion that steepened slopes on uplifted surfaces versus a continuous “erosion of declining slope” that decreased slopes when relief was low. Recent efforts have emphasized the role of hillslope processes that act with channel-forming processes in creating steady-state landscape morphologies (Singh et al., 2015; Sweeney et al., 2015).

Experiments have also focused on channel network growth by seepage erosion. Howard and McLane (1988) allowed groundwater from an adjacent reservoir to move through a package of sediment and exfiltrate through a sloping valley wall. They observed that seepage erosion was strongest at a narrow band where groundwater exfiltrated from the valley wall and undermined the overlying sediment. The overall rate of channel growth by seepage erosion was limited in these experiments by the ability of fluvial transport to remove material from the valley floor after a mass wasting event. Howard (1988) performed similar experiments with slightly cohesive sediment and found that seepage erosion produced narrower and more incised channels. Lobkovsky (2004) showed that seepage erosion is slope-dependent and that beyond a critical slope angle, it can mobilize sediment at slopes less than its maximum angle of stability. Gomez and Mullen (1992) augmented these approaches by using precipitation rather than an adjacent reservoir. They found that headward growth of drainage networks by seepage erosion proceeded in phases similar to what Parker (1977) described for overland flow, but with a different channel morphology. Berhanu (2012) showed that seepage erosion driven by rainfall produced wider, bifurcated channels compared to single, elongated channels produced by groundwater flowing unidirectionally from an adjacent reservoir. The experiments discussed here augment these earlier efforts by investigating the conditions necessary for erosion via surface vs. subsurface flow, with a specific focus on the interplay of overland flow vs. seepage erosion on rates of erosion, integration of NCA, and network expansion in low-gradient landscapes.

### 3. Methodology

#### 3.1 Drainage Network Evolution Experiments

We performed a series of small-scale experiments to simulate the development of drainage networks. The focus of the experiments was to evaluate how precipitation rates and substrate compositions mediate the processes and rates of drainage



network development. To do this, we conducted six experiments where channel development was observed from genesis to full elaboration (10-14 hours) under a range of rainfall rates and substrate compositions [Table 1; Table 2].

Topographic data were captured at discrete time intervals using a FARO Focus 3D terrestrial laser scanner suspended 1 m above the basin. The position of the scanner relative to the basin surface provided point cloud data with a point spacing of 2 mm. The scanner was positioned in the same location for each scan using a computer-controlled cart set on tracks above the basin. Both rainfall and uplift ceased for approximately ten minutes while positioning and capturing each scan.

**Table 1. Experimental conditions, duration, and scan intervals used for each experimental run.**

Run	Substrate Clay Fraction	Rainfall Rate (R)	Uplift Rate (U)	Infiltration Capacity (I)	U/R Ratio	I/R Ratio	Run Duration	Scan Interval
-	weight %	$\mu\text{m/s}$	$\mu\text{m/s}$	$\mu\text{m/s}$	-	-	hr	hr
1	0	11	3.2	210	0.3	19	13	3,2*
2	2	16	3.2	132	0.3	8	10	2
3	2	8	3.2	132	0.4	17	14	2
4	2	16	3.2	132	0.2	8	14	2
5	6	16	3.2	26	0.2	2	14	2
6	6	8	3.2	26	0.4	3	14	2

\*Scan interval of three hours for the first scan and two hours for all subsequent scans

**Table 2. Labels used to refer to the substrate clay fractions and rainfall rates used in experiments.**

Substrate Clay Fraction	Label	Rainfall Rate	Label
weight %	-	$\mu\text{m/s}$	-
0	No Clay	8	Low Rainfall
2	Moderate Clay	11	Moderate Rainfall
6	High Clay	16	High Rainfall

Experiments were conducted in a 0.95 m tall by 0.80 m diameter cylindrical drum designed by Gazzetti (2015) after the apparatus used by Hasbargen and Paola (2000). The drum holds sediment exposed to rainfall and uplift (through base level fall) to generate a drainage network. A 0.02 m wide outlet spans the height of the drum where sediment and water discharge from the basin. A computer-controlled step motor lowers a metal strip at the outlet, dropping base level and instigating channel incision into the substrate. These experiments used a constant uplift rate of 1.15 cm/h that was equivalent to Gazzetti's (2015) "low" uplift rate and slightly faster than Hasbargen and Paola's (2000) rate of 1.00 cm/h [Fig. 2].

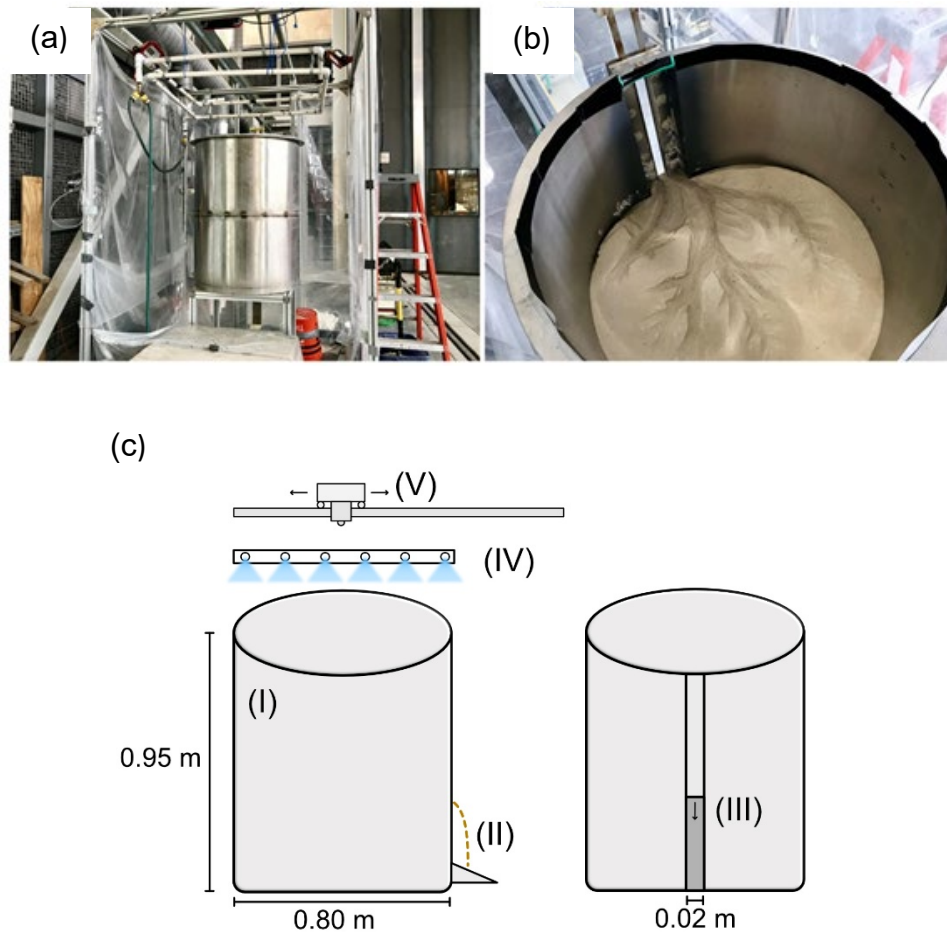


**Figure 2.** (a) Image of the basin with the rainfall simulator suspended above it. (b) Image of the basin's interior after channels developed in the substrate. (c) Schematic of the basin and key features (I-V). (I) The cylindrical basin which holds sediment. (II) Sediment discharge from the basin through the gate. (III) View of the basin facing the gate that allows sediment to discharge and controls base level. (IV) Rainfall source that surrounds the basin on four sides. (V) Movable cart above the basin that houses the terrestrial lidar scanner.

200 The substrate consisted of silica sand ( $d_{50} = 100 \mu\text{m}$ ) mixed with varying amounts of kaolinite clay. Clay both increases cohesion of the substrate and reduces infiltration capacity [Table 1]. The sand and clay were mixed in a cement mixer and sieved to remove any clumps before adding to the basin. Sediment was added to the basin in 5 cm increments, sprayed with a



fine water mist, and compacted by hand with a flat trowel until the sediment package was flat and 25 cm thick. After all the sediment was added to the basin, it was sprayed with a water mist until pooling appeared on the surface, indicating complete saturation of the substrate. By starting with saturated sediment, channel formation by overland flow could begin at the onset of an experiment.

The precipitation source was a set of 20 vegetable misting nozzles suspended 50 cm above the basin on four sides. Precipitation was controlled via a valve outfitted with a gauge that measured water pressure. Pressure was calibrated to specific rainfall rates by measuring the volume of water that fell into the basin over a ten-minute duration. The spatial distribution of rainfall entering the basin varied depending on the nozzle configuration used for an experiment. We measured the spatial variability of rainfall for all nozzle configurations using an array of cups distributed evenly about the basin to measure the volume of water that fell in certain areas. Changing the nozzle configuration was done by covering select nozzles with tape to attain rainfall rates below 16  $\mu\text{m/s}$  while maintaining adequate water pressure for water atomization. A common issue during several experiments was large water droplets contacting the substrate and forming small depressions. This was caused by rainfall coalescing on the cart track above the basin and dripping onto the substrate. The issue was controlled for Run 3 and all subsequent runs using oscillating fans to divert the rainfall away from the tracks. The depressions that do appear in imagery from later runs occurred only at the start of the experiments while an appropriate fan arrangement was established.

### 3.2 Digital Terrain Analysis

Topographic data collected by the lidar scanner were trimmed to the basin area using FARO® SCENE software. Horizontal and vertical alignments of trimmed scans were assessed and corrected, if necessary, using CloudCompare software. Digital elevation models (DEMs) were generated from point cloud data by performing an inverse distance weighted interpolation for each scan with ArcGIS software. Resulting DEMs had 2 mm x 2 mm raster cells and were edited to eliminate cells that included the basin wall. All further topographic analyses of the DEMs were completed using ArcGIS.

The first goal was to differentiate areas contributing surface water to channels, contributing areas (CAs), from internally-drained non-contributing areas (NCAs). A combination of filled DEMs (i.e., internally-drained cells or “sinks” eliminated) and unfilled DEMs were used to perform this analysis in four steps [Fig. 3]. First, the “Sink” tool identified cells on unfilled DEMs where surface water flow terminates in internally-drained depressions rather than an outlet. “Sink” identifies cells that do not drain to the edge of the DEM, which it assumes to be an outlet. A limitation to this approach is that cells draining to the basin’s edge, other than the outlet, remained unclassified. If sink cells occurred in an area where a channel was visually present, they were assumed to be within the noise of the lidar data and were removed. After locating sink cells, their watersheds were delineated with the “Watershed” tool, providing the total NCA as raster cells converted to polygons. Third, all potential CA was identified using the “Basin” tool on a filled DEM that showed theoretical watershed polygons for all channels if the basin was void of NCA. Channels with watersheds that formed along the edge of the basin were eliminated as their formation was



driven by the focused water flow along the basin wall rather than natural processes. Fourth, CA polygons were trimmed where they overlapped with NCA polygons to provide a final CA for all channels in the basin. The results from this analysis were sequential scans showing the total surface water CA and NCA in the basin as defined by the topography [Fig. 3].

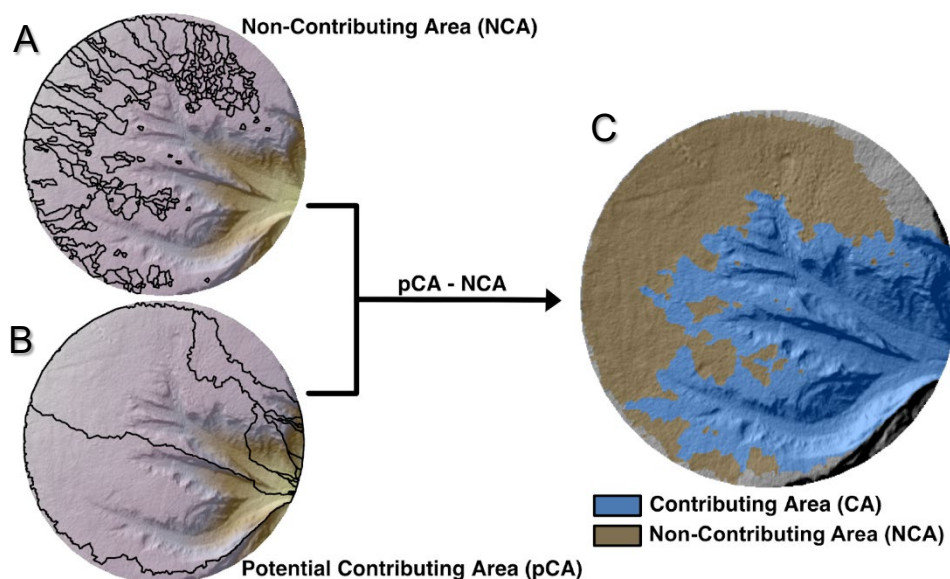


**Figure 3. Process of generating contributing area (CA) and non-contributing area (NCA) from a DEM. (A) Delineation of NCA on the upland surface where each polygon is the watershed of an internally-drained depression. (B) Delineation of potential CA where each polygon is the watershed of a channel. Note CA polygons of channels that formed along the edge of the basin were removed. (C) Result of differencing the CA polygons that overlap with NCA polygons to provide a final CA polygon for each watershed.**

The delineated CA included two distinct components: (1) channelized area and (2) non-channelized upland area that supplied water to the channel heads. To isolate the two CA components, we first created elevation contour lines using the “Contour” tool on an unfilled DEM with a contour interval of 0.001 m. By selecting contour lines from different elevations and creating small joining segments by hand, a single contour that approximately outlined the channelized extent of the drainage network was created. This single contour line was used to split the CA polygons into “upland CA” and “channelized CA” components at each timestep of a run. Some channel heads were too small-scale for elevation contour lines to capture, but this methodology provided enough precision to approximate the area of each component.



250 The experiments produced two distinct channel head morphologies: Type 1 and Type 2. Type 1 channel heads were v-shaped with low slope and low relief headwalls. Type 2 channel heads were amphitheater-shaped with high slope and high relief headwalls. To identify when and where each head type was present, we extracted slope and local relief values from characteristic channel heads across multiple timesteps and experiments. The values were extracted from a 2 mm buffer around a line drawn along the channel head perimeter. The buffer direction was directed towards the valley to exclude upland areas.

255 These values were used to classify cells throughout the basin as either “Low Slope & Relief” or “High Slope & Relief,” which corresponded to values extracted from Type 1 and Type 2 channel heads, respectively [Table 3].

**Table 3. Slope and local relief values extracted from Low Slope and Relief (Type 1) and High Slope & Relief (Type 2) channel heads.**

Statistic	Low Slope & Relief		High Slope & Relief	
	Relief <i>m</i>	Slope <i>degree</i>	Relief <i>m</i>	Slope <i>degree</i>
(+1) Std. Dev.	0.0026	24.7	0.0085	53
Average	0.0017	16.6	0.0049	25
(-1) Std. Dev.	0.0008	8.4	0.0013	17.1

260

Cells were classified as “Low Slope & Relief” when their slope was less than 24.7 degrees and greater than 8.4 degrees and local relief less than 0.0026 m and greater than 0.0008 m. Cells were classified as “High Slope & Relief” when they had a slope greater than 17.1 degrees and relief greater than 0.0013 cm [Table 2]. Approximately 15% to 40% of “Low Slope & Relief” cells overlapped with cells also classified as “High Slope & Relief” for each scan. The overlapping cells were

265 categorized as “Low Slope & Relief” because they often occupied rougher areas near the valley bottom where most adjacent cells shared the same classification.

By observing the relief and slope classification of cells at channel heads, we assigned a dominant channel type, Type 1 or Type 2, to each sub-watershed (i.e., CA polygon). Channels were classified as Type 1 when cells at the channel head had a “Low Slope & Relief” classification, while channels were classified as Type 2 when cells at the channel head had a “High Slope & Relief” classification. Many channel heads had adjacent cells from both slope and relief categories, which complicated the task of assigning a dominant channel type. Channels were classified as Type 2 when all cells at channel heads had a “High Slope & Relief” classification. An additional line of evidence for process classification was the planview geometry of drainage networks. Type 1 channels often formed branching, dendritic networks while Type 2 channels formed a single wide valley.

270

With watersheds classified by the dominant channel type, we calculated the amount of erosion associated with each type. To

275 do this, we calculated the depth of sediment eroded by subtracting DEM elevation values from sequential timesteps. The



volume of sediment removed was then calculated by multiplying the change in depth by the raster cell size of  $4 \text{ mm}^2$ . Only the channelized area polygons were used to aggregate the volume of sediment removed as non-channelized areas often had small amounts of change (mean of  $\approx 0.001 \text{ m}$ ) likely caused by both the lidar unit's ranging error of  $\pm 0.002 \text{ m}$  and small amounts of sediment diffusion across the upland surface. Any positive values were assumed to be within the lidar data ranging error and set to a value of zero.

## 4. Results

### 4.1 Channel network expansion

Channel network growth resulted in decreasing NCA through time as upland area was captured by the drainage network, converting NCA to CA [Fig. 4]. The initial surface was void of channels, and precipitation was routed to small internally-drained depressions exclusively. Once channel development began, NCA was integrated into the drainage network as channel heads extended into the uplands and breached shallow drainage divides of the depressions. Channels also integrated NCA when their valleys widened via mass wasting. By the conclusion of most experiments, channels had reached their maximum extent and nearly the entire basin surface was CA. In most runs, channel development accelerated at the beginning, remained at a constant rate for a majority of the time, and then slowed near the experiment's conclusion when the basin was near full integration [Fig. 4].

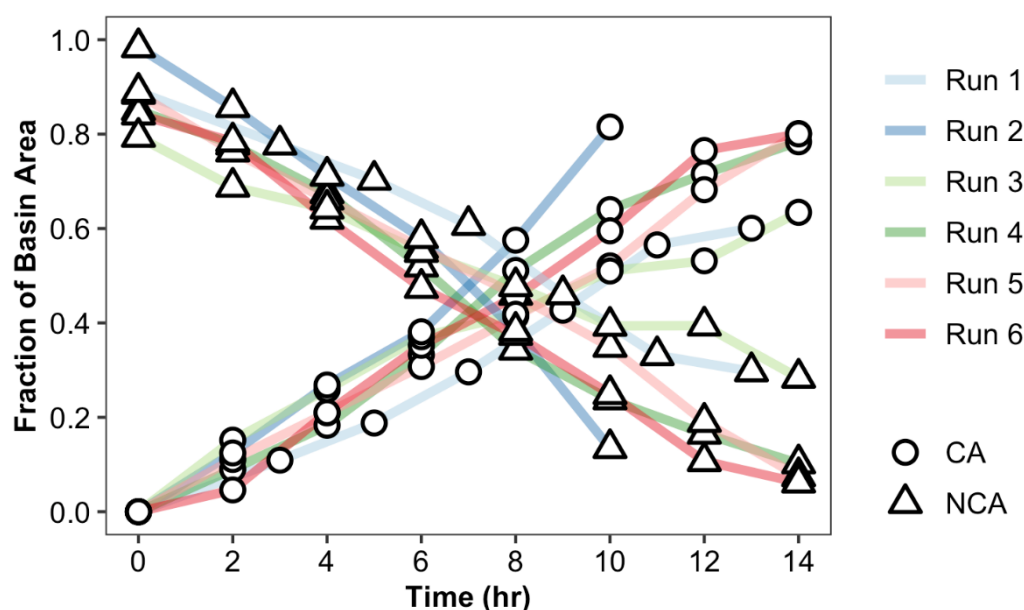




**Figure 4. Time-series of the contributing area (CA) and non-contributing area (NCA) of each experiment. CA and NCA are normalized by basin area.**

295 To investigate the impacts of different experimental conditions, we isolated the effects of a single condition by averaging multiple experiments with the same substrate, but different rainfall rates (and vice versa) [Table 2]. Run 1 and 2 were excluded from these analyses because they had run durations, scanning intervals, substrate compositions, or rainfall rates that precluded comparison with other experiments in these analyses. All experimental conditions followed a similar temporal pattern and did not produce statistically significant differences in mean NCA integration rate [Fig. 5]. NCA integration rates rose early in the  
 300 experiments and then slowly decreased, ending at just under 5% of the basin area integrated per hour.

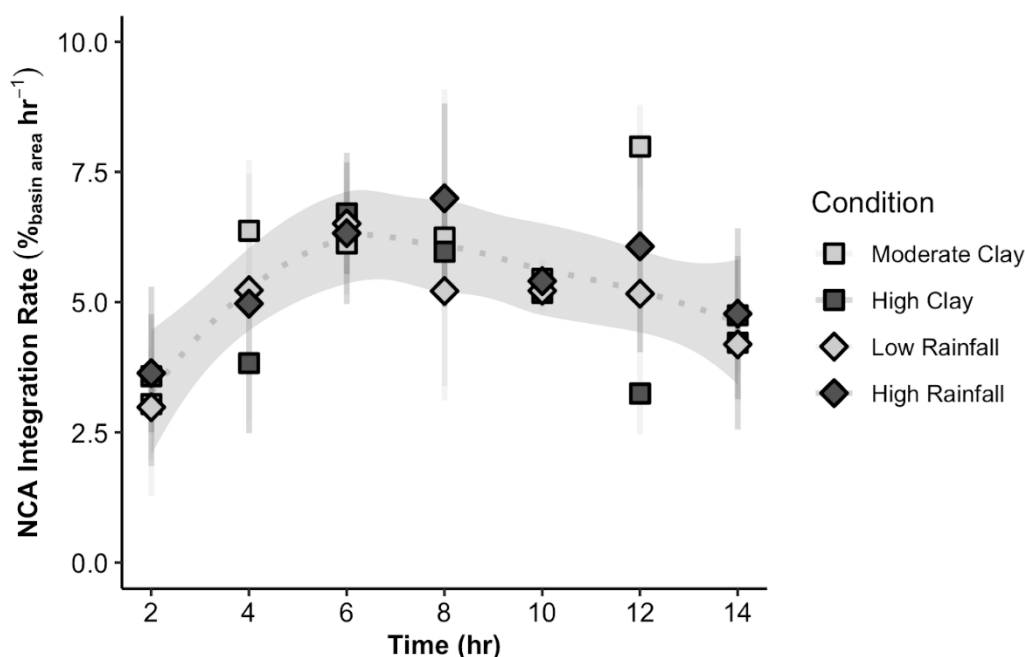


**Figure 5. Average NCA integration rates through time per experimental condition. Error bars are the standard deviation between experiments at equivalent timesteps. The shaded area is the 99% confidence interval of a locally weighted smoothing regression curve of the average values.**

305



## 4.2 Types of Channel Development

All experiments had two types of coevolving channel development that were differentiated by their morphology. Type 1 channels had dendritic drainage patterns with gently sloping first-order channel heads, while Type 2 channels had single high relief channel heads. We interpret these as developing from overland flow vs. seepage, respectively, and elaborate on this interpretation in the discussion section. At the onset of experiments, overland flow channel heads formed near the basin outlet where a constant base level fall caused channel incision. As knickpoint migration eroded into the basin uplands, channels bifurcated and formed first-order channel heads. After these channels had established a drainage network during the first six to eight hours of an experiment, seepage erosion began. The largest seepage-driven channels formed when mass wasting of channel heads began to increase in frequency and magnitude, causing the channel to attain an amphitheater morphology [Fig. 6]. Drainage divide collapse and channel coalescing eliminated some of the smaller seepage channels, while the larger channels often persisted until the conclusion of the experiment.

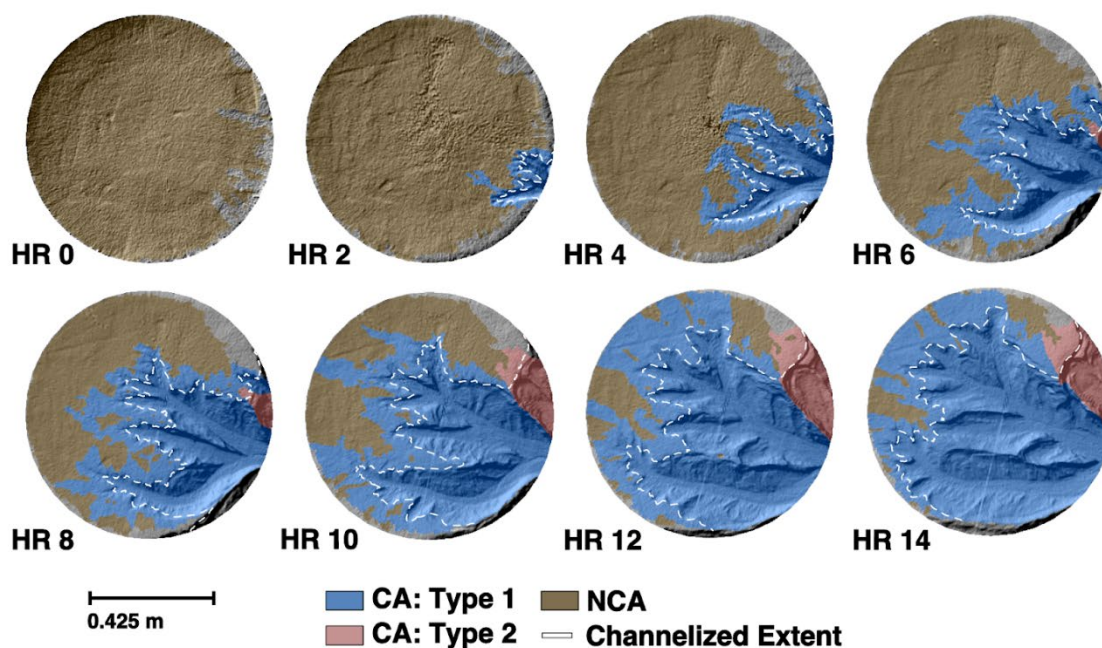
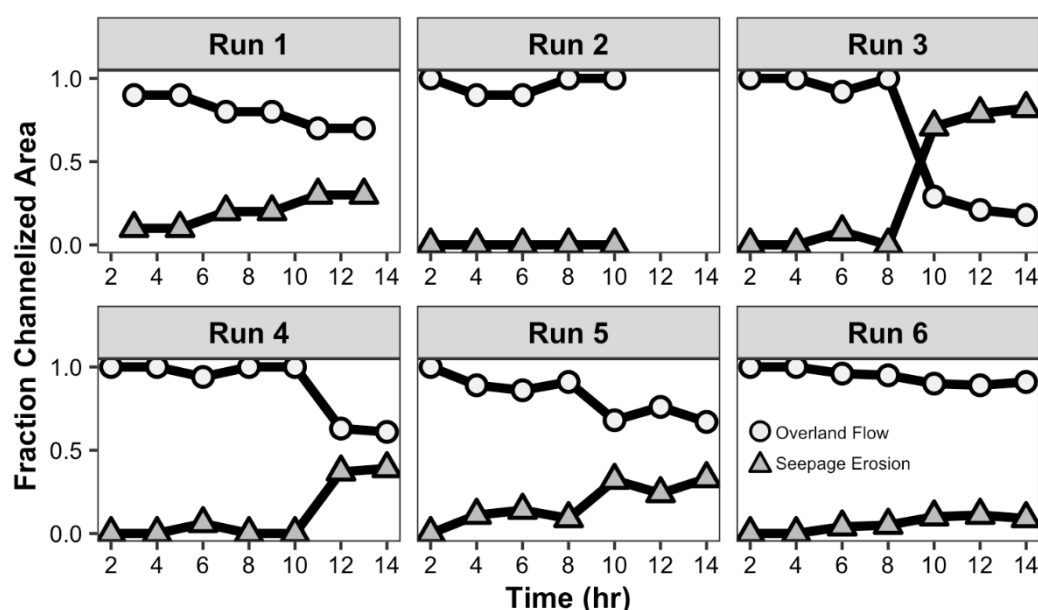


Figure 6. Example of classifying CA polygons as Type 1 from overland flow erosion (blue) or Type 2 from seepage erosion (red) at each timestep for an experiment. The channelized extent (white dashed line) approximately separates the CA polygons into upland CA and channelized area components.



Each experiment had varying amounts of each type of channelization over its duration. Overland flow channels, on average, comprised a majority of total channelized area for most experiments and were dominant during the first half of all experiments. After hour 8, some experiments had a sharp decrease in channelized area from overland flow after these channels transitioned to seepage channels between timesteps [Fig. 7]. The largest of such decreases occurred during Run 3, which was the only experiment where seepage channels obtained a majority of the channelized area. Run 6 was notable for maintaining the largest average fraction of overland flow-driven channels, with 95% of total channelized area, over the experiment's duration. Run 1 was the only experiment where seepage erosion began at the experiment's onset and channelized a substantial area before hour 8.



**Figure 7. The fraction of total channelized area with channel head erosion driven by overland flow and seepage erosion through time.**

Analysis of the results by parameter showed the consistency of type of channel development was affected by both the substrate composition and rainfall rate [Fig. 8]. High clay experiments had a greater and more consistent amount of overland flow channelization compared to moderate clay experiments. For high clay experiments, channelized area from overland flow increased linearly through time at a rate of  $0.03 \text{ m}^2 \text{ m}^{-2} \text{ h}^{-1}$  and reached a maximum of  $0.42 \pm 0.05 \text{ m}^2 \text{ m}^{-2}$  by hour 14. Reported



channelized areas are normalized by basin area. The average standard deviation of overland flow channelized area for high  
 340 clay experiments was  $0.02 \text{ m}^2 \text{ m}^{-2}$ , four times less than moderate clay experiments. Seepage channels proliferated under  
 moderate clay conditions, with most growth in channelized area from seepage erosion coming after hour 8.

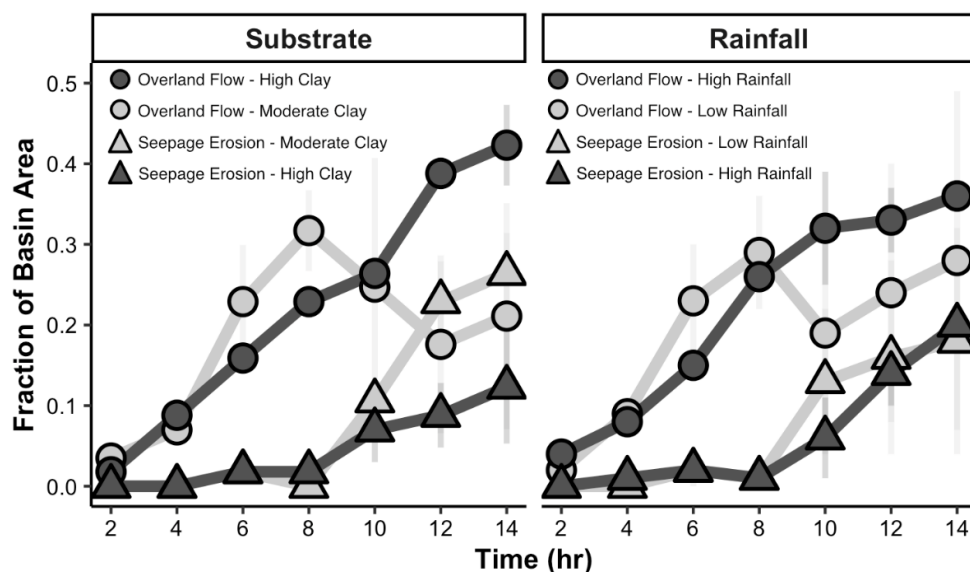
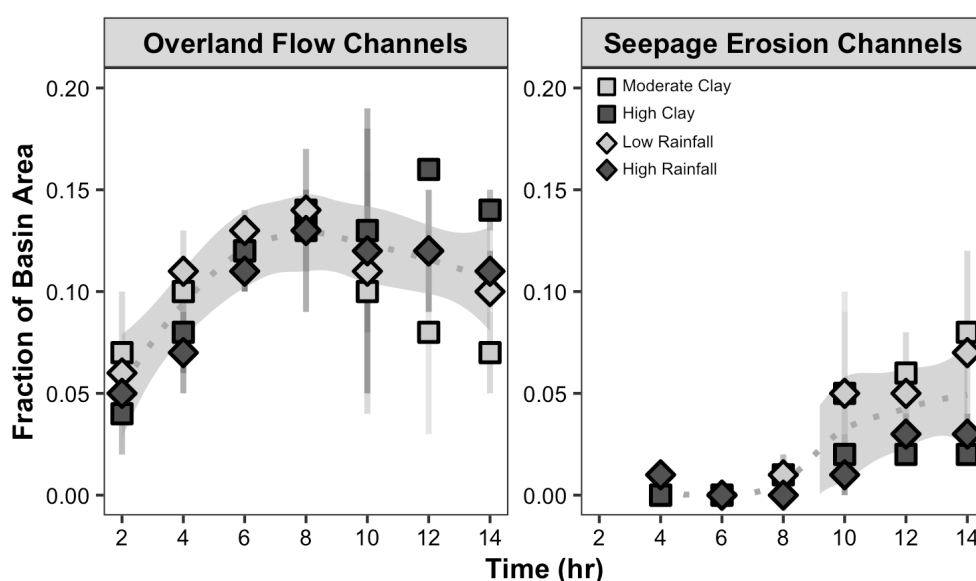


Figure 8. Average channelized area of overland flow and seepage channels normalized by total basin area through time for  
 experiments with moderate or high clay substrate (left) and low or high rainfall (right). Error bars are the standard deviation in the  
 345 channelized area between experiments at each timestep. Area values are normalized by total basin surface area.

On average, high rainfall rates resulted in greater and more consistent channelized areas of both channel types, but particularly  
 for channel heads eroding through overland flow. High rainfall rate experiments led to a linear increase in channelization by  
 overland flow through time, reaching a maximum normalized channelized area of  $0.36 \pm 0.02 \text{ m}^2 \text{ m}^{-2}$  at hour 14. The average  
 350 standard deviation of channelized area by overland flow in the high rainfall runs,  $0.03 \text{ m}^2 \text{ m}^{-2}$ , was three times less than low  
 rainfall rate experiments. Low rainfall rate experiments also differed in that channelized area from overland flow decreased  
 between hour 8 and 10 as more channels transitioned to seepage channels. However, unlike the moderate clay experiments,  
 the decrease was not as sustained; channelization by overland flow continued to increase from hour 10 onwards. Rainfall rates  
 appeared to have less of an influence on the total area of seepage channelization. The main difference was the variability in  
 355 channelized area: high rainfall rates had an average standard deviation of  $0.02 \text{ m}^2 \text{ m}^{-2}$  compared to  $0.05 \text{ m}^2 \text{ m}^{-2}$  for low rainfall  
 rates.



Temporal changes in upland CA that supplied water to channel heads via surface flow followed a similar pattern to NCA integration rate through time [Fig. 5, 9], rising initially, then decreasing slowly over the remainder of the experiment. Under all conditions, overland flow channels had a greater average upland CA,  $0.11 \text{ m}^2 \text{ m}^{-2}$ , compared to seepage channels,  $0.02 \text{ m}^2 \text{ m}^{-2}$ . The large standard deviations around hours 8 to 10 correspond with the onset of seepage erosion in many experiments. Seepage channels that formed by transitioning from overland flow channels under moderate clay and low rainfall conditions accounted for a majority of the variance.



**Figure 9.** Upland CA of overland flow (left) and seepage (right) channels through time for different experimental conditions. Averages at each time step are plotted, with error bars indicating the standard deviation between experiments. The shaded area is the 99% confidence interval of a locally weighted smoothing regression curve of the average values. Contributing area values were normalized by the total basin surface area.

### 4.3 Erosion

Channel networks expanded, eroding sediment from an increasing fraction of the basin through time. Areas in the basin prone to erosion include channel heads, valley floors, and valley walls. Low magnitude erosion occurred along the valley floor, where the erosion depth between timesteps was on the order of one to two centimeters. The highest magnitude of erosion occurred at valley walls and drainage divides by mass wasting, which could remove multiple centimeters of sediment in a single event [Fig. 10].

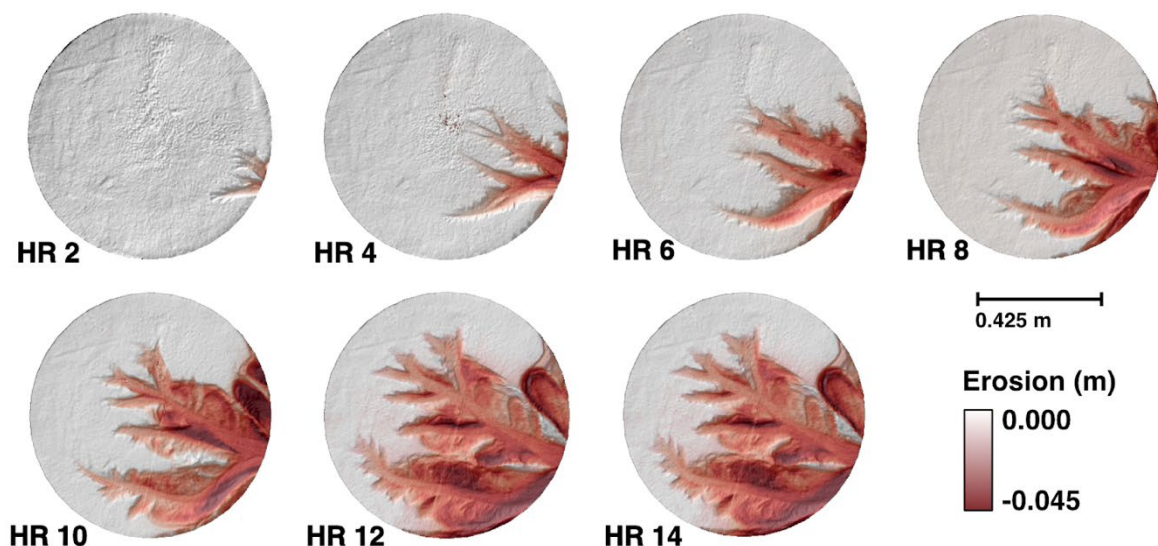


**Figure 10. DEM time-series of erosion depth per timestep throughout Run 5. Red (negative) indicates erosion.**

Erosion volumes increased through time for all experiments; however, the total erosion volume differed between experiments. We assessed the erosion of each channel type independent of duration and channelized area by calculating incision rates (erosion volume divided by the channelized area) and then normalizing by the rate of base level fall. Erosion rates that perfectly match the rate of base level fall would be equal to 1. For all experiments, average incision rates of seepage channels were greater than overland flow channels [Fig. 11].

The incision rate of overland flow channels increased during the early period of channel establishment, then equilibrated at a value about half of the rate of base level fall, 0.46 on average. An exception to this pattern of equilibration was Run 5 which had a drainage divide collapse between hours 12 and 14 causing a sharp rise in incision rate. Seepage channels had fewer incision rate observations than overland flow channels because they formed later in the runs and were sometimes eliminated by drainage divide collapse. The incision rates associated with seepage channels were closer to the rate of base level fall, 0.83 on average. Run 1 had an exceptionally high incision rate for seepage channels, equilibrating at 0.98, a value greater than all other experiments and nearly equivalent to the rate of base level fall.

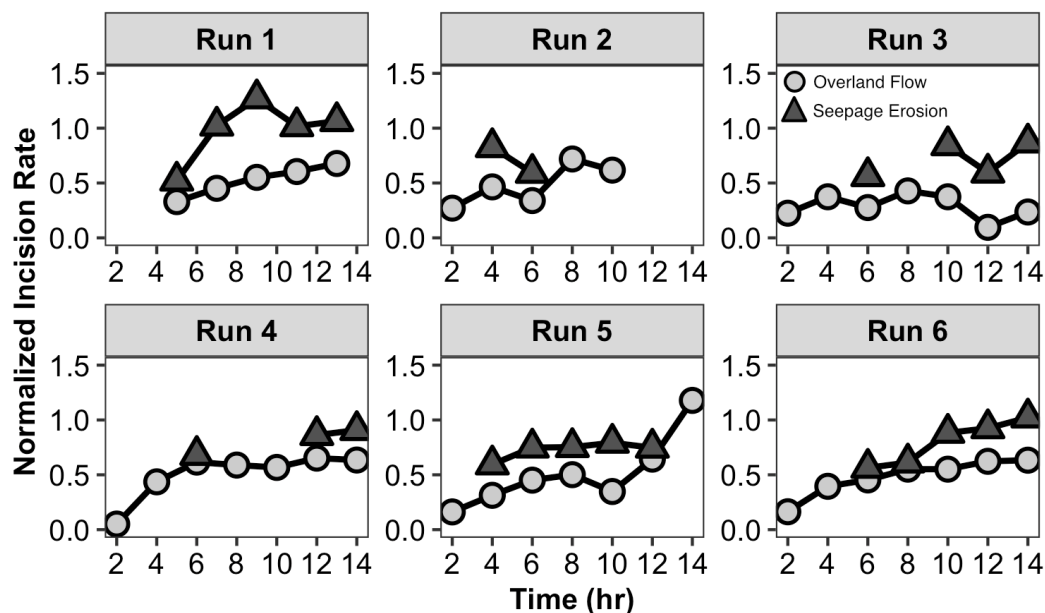
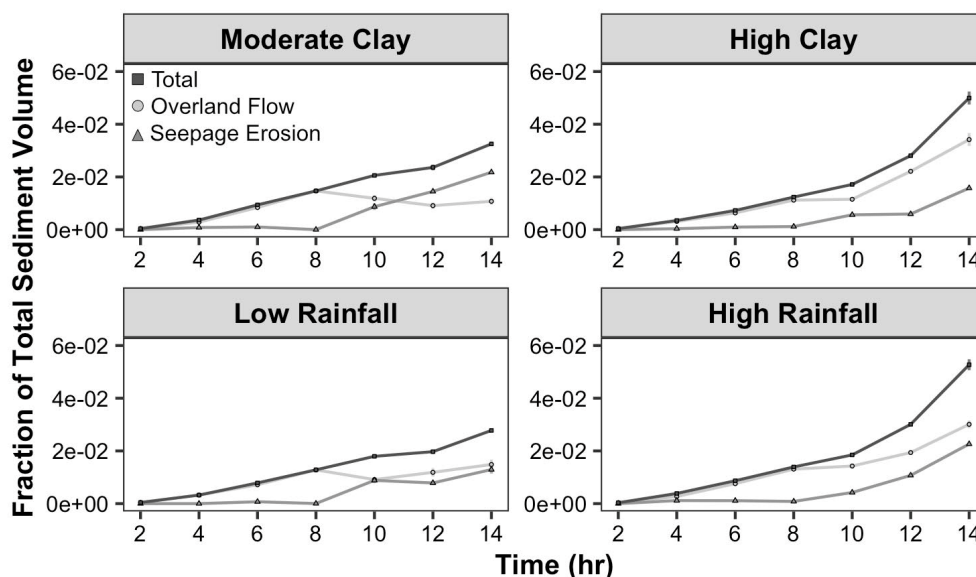


**Figure 11. Normalized incision rates of overland flow (circles) and seepage (triangles) channels throughout each experiment. A normalized incision rate of 1 indicates that the incision rate equals the rate of base level fall.**

In terms of the total erosion, experiments with conditions that led to greater amounts of channelization, high clay and high rainfall [Fig. 8], eroded at higher rates and in larger volumes than other conditions [Fig. 12]. High clay experiments had more erosion primarily from overland flow channelization [Fig. 8], while high rainfall experiments had a greater contribution from both types of channels. Under conditions with more channelization from seepage, such as moderate clay and low rainfall [Fig. 8], seepage channels eroded similar or greater volumes of sediment than overland flow channels. In all cases, seepage channels were only a substantial erosion source after hour 8. The sudden rise in erosion volumes between hour 12 and 14 for high clay and rainfall experiments was due to the drainage divide collapse during Run 5. However, even when Run 5 was excluded from the final timestep average, the high clay and rainfall experiments still maintained greater erosion rates and volumes than the other conditions.



405 **Figure 12.** Average erosion volume of overland flow and seepage channels under different experimental conditions per timestep. The  
 “Total” erosion volume is the sum of both erosion values per timestep. Error bars are the standard deviation in erosion volume  
 between experiments.

## 5. Discussion

410 The experiments described here focus on drainage evolution on a low-gradient surface subjected to a constant supply of rainfall  
 and base level fall. These conditions are not unique to our experiments. Base level changes are common in post-glacial  
 environments, associated with processes like glacial lake drainage, valley incision from high discharge glacial meltwater  
 events, or differential uplift associated with isostatic rebound. Although many of these incisional triggers are abrupt, the upper  
 watershed experiences base level fall as a more continuous process as incision propagates upstream, similar to the experiments  
 415 here. For example, incision of the Minnesota River valley by glacial meltwater has led to progressive and on-going drainage  
 extension and incision into relatively flat-lying glacial tills and glaciolacustrine sediments in southern Minnesota (Gran et al.,  
 2009, 2013) [Fig. 13]. Likewise, drainage of major glacial lakes like glacial Lake Duluth lowered base level to streams draining  
 into Lake Superior by over 200 meters (Grimaud et al., 2016), leading to incision that continues to migrate upstream over time  
 [Fig. 13]. Incisional waves associated with base level fall are driving network extension in similar watersheds across large  
 420 swaths of the Central Lowlands, and the experimental results here give additional insight into the processes driving network  
 expansion and which conditions favor overland flow vs. seepage erosion.

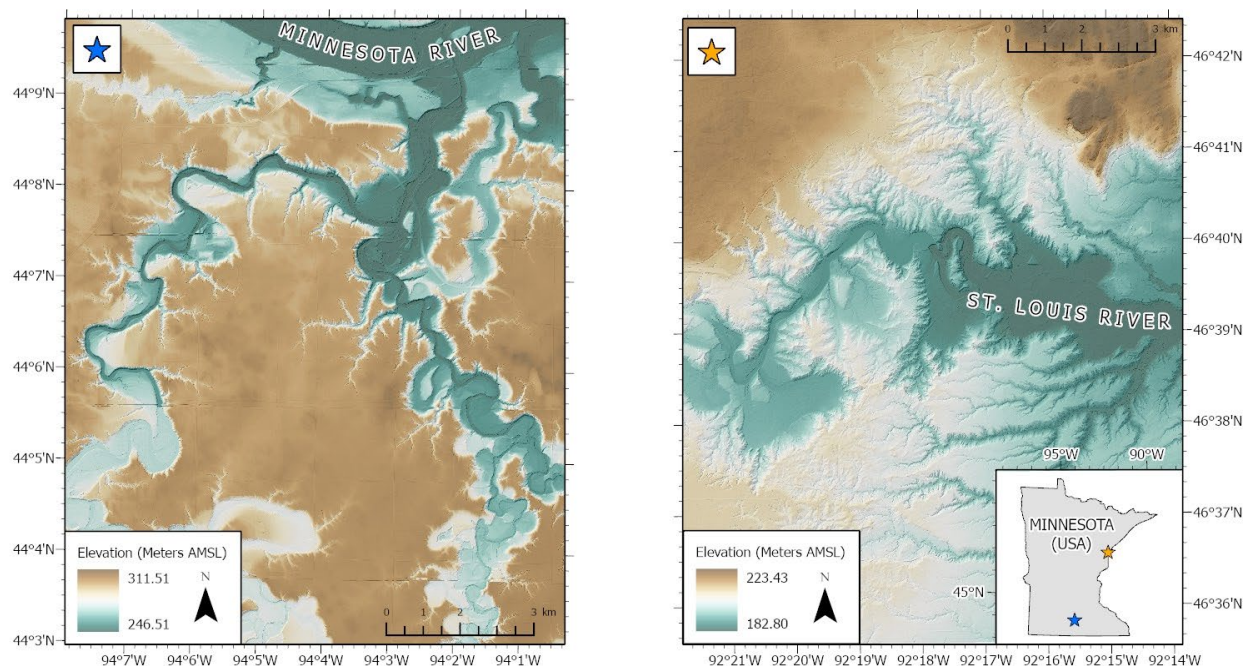


**Figure 13. DEMs of Minnesota River tributaries in south-central Minnesota and tributaries to the St. Louis River in northeastern Minnesota. In both cases, tributaries incised after a base level drop at their outlet and continue to erode headward into the surrounding uplands.**

## 5.1 Channel Development Processes

Our experiments demonstrate that channel development driven by relative base level fall can produce two distinct and coevolving channel types that differ in their morphology and hydrologic characteristics. We attributed these differences to be the result of separate channel-forming processes. Type 1 channels, characterized by large upland CAs and low relief channel heads, formed by overland flow where surface water accumulated as it moved downslope and exerted shear stresses high enough to erode the substrate [Fig. 8]. Overland flow was an active process early on, and as upland CA increased through time, incision rates from overland flow also increased [Fig. 8, 9]. The large upland CA supported numerous first-order channels, creating dendritic drainage patterns with slowly increasing total erosion volumes as observed in other experiments focused on overland flow channel development (Hasbargen and Paola, 2000; Parker, 1977; Pelletier, 2003) [Fig. 6].



Type 2 channels formed by seepage erosion where groundwater exfiltrated through channel headwalls with enough force to entrain sediment and cause mass wasting by undermining headwalls. The intermittent nature of mass wasting events caused headward erosion of channels to proceed as large, sporadic failures unlike the consistent cadence of headward erosion by overland flow. The small upland CA of seepage erosion channels supplied less surface water to channel heads, hindering  
 440 overland flow and allowing seepage erosion to initiate mass wasting which formed high slope and relief headwalls [Table 3]. Both experiments (Berhanu et al., 2012; Gomez and Mullen, 1992; Howard, 1988; Howard and McLane, 1988) and studies in natural landscapes (Abotalib et al., 2016; Kochel and Piper, 1986; Laity and Malin, 1985; Schumm et al., 1995) have identified amphitheater-shaped headwalls as a common, though not exclusive (Petroff et al., 2011), feature of seepage erosion.

## 5.2 Process Drivers: Substrate, Precipitation, Relief

445 The degree to which drainage networks develop by overland flow or seepage erosion depends on a number of factors including substrate, rainfall rate, and relief. Field studies in unconsolidated sands and gravels have found that groundwater seepage can play an important role in channel development and formation (Coelho Netto et al., 1988; Dunne, 1990; Lapotre and Lamb, 2018; Micallef et al., 2021; Pillans, 1985; Schumm et al., 1995; Schumm and Phillips, 1986; Uchupi and Oldale, 1994). As grain size decreases to silt and clay size fractions, low permeability limits infiltration, decreasing the likelihood of seepage  
 450 erosion and sapping (Lapotre and Lamb, 2018). Results from our experimental runs are compatible with these field observations; the degree to which drainage networks developed by overland flow or seepage erosion varied as a function of substrate composition. Infiltration tests found that differences between the high clay and low clay experiments [Table 1] effectively straddled conditions for seepage erosion feasibility as laid out in Lapotre and Lamb (2018), with high clay experiments approaching conditions where seepage was not possible, while low clay experiments still allowed for seepage  
 455 erosion to occur. Experiments with a low or moderate clay substrate had both larger infiltration capacities that allowed more water to infiltrate into the subsurface and lower cohesion, making it easier for seepage erosion to occur [Table 1; Fig. 8 & 9].

The connection between erosion process and rainfall rate is more complicated. In order for channel heads to erode by seepage erosion, there must be enough precipitation that the infiltrating fraction can provide the discharge needed to overcome cohesion holding particles in place. Field studies by Micallef et al. (2021) in a series of coastal gullies in New Zealand, for example,  
 460 found a rainfall threshold of 40 mm/day necessary for seepage erosion to occur. Experimental studies find that the velocity of exfiltrating groundwater also must be high enough to remove the eroded particles deposited at the base of slopes, setting up the headwall for continued erosion (Abrams et al., 2009; Howard and McLane, 1988; Onda, 1994). For erosion by overland flow, there must be enough discharge on the surface to generate a high enough shear stress for particles to be eroded and transported downstream. Thus, high precipitation and high contributing area both contribute to greater erosion via overland  
 465 flow. High rainfall rates coupled with high clay contents had the highest erosion volumes overall [Fig. 12] and were particularly amenable to overland flow over seepage erosion as less of the precipitation that landed on the surface was lost to infiltration. Unlike Berhanu (2012), both elongated, single channels and wide, bifurcated channels formed by seepage erosion



under uniform rainfall, suggesting that groundwater flow was influenced by other factors like the presence of adjacent channels or the model boundary to maintain uniform flow to channel heads (Cohen et al., 2015).

470 In addition to substrate composition and rainfall rate, relief generated by channel incision was an important control on seepage erosion. During the initiation and early expansion of the drainage network, relief was limited, and only a few channels formed by seepage erosion as channel heads competed for upland CA. The dominant channels captured enough upland CA to evolve by overland flow, while the subordinate channels were starved of upland CA and could only grow by seepage erosion. These early seepage erosion channels were often eliminated through time as mass wasting breached small drainage divides, and  
 475 seepage channels were incorporated into larger channel networks. Later in the experiments, some channel heads became starved of upland CA, and existing channels underwent a process transition from erosion via overland flow to seepage erosion. The earliest evidence of process transition appeared around hour 6 of most experiments. During this time, the morphology of some overland flow channels began acquiring an amphitheater shape as the frequency of headwall mass wasting increased. The resulting amphitheater shape had a smaller upland CA. Substantial amounts of mass wasting occurred after hour 8 when  
 480 seepage erosion could consistently undermine headwalls. By that time, all experiments had experienced 9.2 cm of total uplift, and relief throughout the basin had increased as channel incision progressed in unison. The greater relief likely exceeded a critical slope stability threshold, and seepage erosion was capable of initiating mass wasting like the experiments by Lobkovsky (2004) demonstrated. Pelletier (2003) similarly noted that as relief increased during their experiments, base flow (i.e., groundwater) became an increasingly important driver of channel growth.

### 485 **5.3 Network expansion and erosion over time**

In an evolving post-glacial landscape, NCA extent starts high and declines through time as channel networks evolve and drainage density increases (McDanel et al., in prep.; Meghani et al., in prep.). In our experiments, NCA integration rates did not differ significantly between experimental conditions despite causing varying amounts of overland flow and seepage erosion channelization [Fig. 5, 7]. Part of this was related to the dominance of overland flow overall and particularly during the first  
 490 half of the experiments, when relief was low. In Run 3, where seepage erosion was the dominant erosional process for multiple hours, NCA integration slowed, which indicates that channel network expansion could slow over time as declining CA and increasing relief allow for more seepage erosion to occur.

In terms of erosion, overland flow accounted for the majority of the erosional volume in most experiments [Fig. 12], but the rate of incision was higher in areas eroding through seepage erosion [Fig. 11]. Overland flow channels were characterized by  
 495 slow, consistent erosion of valley floors through time with occasional mass wasting of steep valley walls. Individual channels had limited erosional power and incised through the substrate at an average rate about half the rate of base level fall [Fig. 11]. The incision rate did not differ substantially between experiments [Fig. 11]. Overland flow accounted for the majority of erosional volume in most experiments because it channelized larger areas that cumulatively eroded more sediment. It followed



that conditions favoring overland flow channelization - high clay and rainfall - were associated with the largest erosion volumes  
 500 [Fig. 8 & 12].

Seepage erosion caused mass wasting, which often removed multiple centimeters of headwall sediment in a single event. The large magnitude of erosion by mass wasting resulted in incision rates greater than overland flow that nearly kept pace with the rate of base level fall [Fig. 11]. In runs with conditions that favored seepage erosion, erosional volumes from seepage were similar to volumes eroded via overland flow in the latter half of the experiments, when seepage erosion was more dominant  
 505 [Fig. 12]. Run 1 had particularly high incision rates; the less cohesive substrate in Run 1 increased the effectiveness of seepage erosion relative to other experiments. However, seepage erosion caused mass wasting episodically over a small area for most experiments compared to the area eroded through overland flow, which limited the total volume of sediment eroded by seepage. Mass wasting was episodic because of the time needed for exfiltrating groundwater to undermine channel headwalls. Like the experiments by Howard and McLane (1988), numerical modeling by Abrams et al. (2009), and observations in the field by  
 510 Onda (1994), sediment deposited at the base of headwalls after mass wasting had to be removed for erosion to proceed. Deposits that are not removed can temporarily stabilize slopes until fluvial transport or overland flow removes them, which can slow the rate of channel evolution.

#### 5.4 Implications for Drainage Network Development

Different models of drainage network development (e.g., top-down versus bottom-up) can explain how hydrologically-  
 515 disconnected areas, NCAs, are gradually integrated into the drainage network over time. The experiments presented here explored processes associated primarily with a bottom-up model of drainage network integration driven by relative base level fall, which has been associated with low-gradient settings like plateaus (Whipple et al., 2017), tidal marshes (D'Alpaos et al., 2005, 2007; Fagherazzi et al., 2012), and formerly glaciated landscapes across the Central Lowlands (Gran et al., 2009, 2013). The experiments demonstrate that drainage network development driven by base level fall could proceed by different processes  
 520 depending on the substrate composition, rainfall intensity, and relief generated by channel incision.

A critical finding was that the dominant process of channel development can transition from overland flow to seepage erosion as channel incision creates more relief over time. The degree of channel incision depends on both the magnitude of base level drop and the amount of time incision has had to propagate through the drainage network. Newly developing rivers may not exceed the relief threshold for seepage erosion to consistently cause mass wasting, restricting headward erosion to overland  
 525 flow. More incised rivers may have generated enough relief to become susceptible to routine mass wasting by seepage erosion, changing the dominant process of headward erosion. The onset of seepage erosion may be particularly important when considering the susceptibility of a landscape to gullyng, which seepage erosion can drive and is a major source of land degradation in many low-gradient settings used as agricultural land (Castillo and Gómez, 2016; Poesen et al., 2003; Valentin et al., 2005). Seepage erosion also allows network expansion to continue even if upland CA is too low for overland flow to

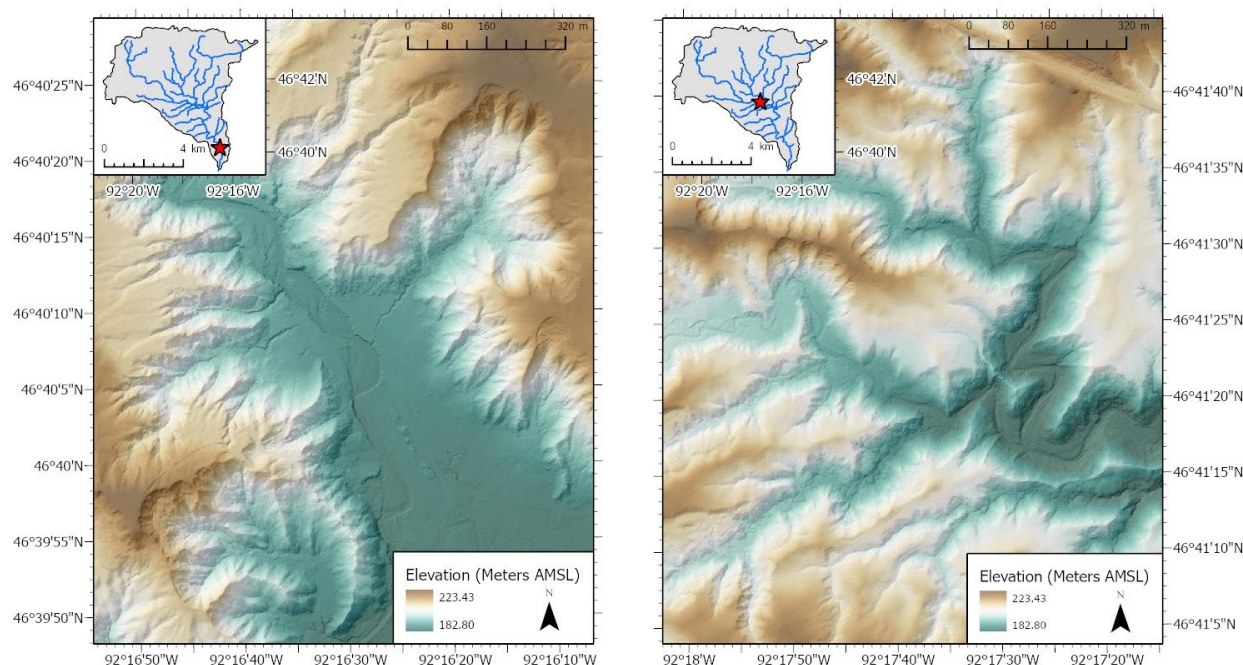


530 exceed erosional thresholds at the channel heads. This could be quite important in disconnected post-glacial landscapes with significant areas in NCA.

The processes of channel development could also affect the pace of NCA integration in low-gradient landscapes. Our experiments suggest if conditions support erosion by overland flow, then channels may integrate NCA at a consistent rate after an early period of channel initiation. Channels developing by seepage erosion tend to integrate less NCA, which could reduce the overall rate of NCA integration depending on the pervasiveness of seepage erosion within a drainage basin. However, even though seepage erosion integrated NCA at a slower rate, incision rates were higher from seepage erosion, and volumetric erosion rates can be similar under both processes.

Our analysis assumed that precipitation routed from a topographically-defined CA drove channel development. This assumption might be incorrect if NCA depressions filled with water and overtopped their drainage divides or if groundwater from NCA crossed surface divides to reach channels during the experiments. Lai and Anders (2018) demonstrated that such hydrologic connections between NCA and drainage networks are critical in driving channel development in low-gradient post-glacial landscapes. While the experiments did not account for NCA connections, they underscored how the hydrologic pathway by which potential connections occurred could influence the processes of channel development and the resulting channel morphology.

545 In light of these findings, we have focused on the implications for drainage networks in the glaciated Central Lowlands region, USA, that developed in a largely low-gradient setting with different glacial deposits, climate regimes, and degrees of channel incision. Along a tributary of the St. Louis River in northeast Minnesota, USA, we observed where relief is potentially driving different processes of channel development [Fig. 14]. Many channels located in the lower watershed have amphitheater-shaped headwalls indicative of seepage erosion and mass wasting, which differ from those in the upper watershed that have channel tips more characteristic of overland flow. The outlet of Mission Creek has experienced several base level adjustments associated with changes in the water level of Lake Superior, causing incision to propagate into the uplands (Grimaud et al., 2016). Channels in the lower watershed are proximal to the outlet and have more relief. Additionally, the lower watershed has a substrate of sandy to clayey lacustrine sediment overlying sedimentary bedrock while the upper watershed has clayey glacial till that lacks well-defined lateral flow paths through permeable substrate (Lusardi et al., 2019). The combination of high relief, less cohesive, and more permeable sediment in the lower watershed favors mass wasting induced by seepage erosion. While Mission Creek is not necessarily prototypical of post-glacial rivers elsewhere in the region, it is an illustrative example of how overland flow and seepage erosion may operate within a watershed simultaneously, impacting the processes by which drainage networks expand.



560 **Figure 14. Comparison of channels in the lower (right) and upper portion (left) of the Mission Creek watershed in Fond du Lac, MN.**

The experiments also showed that substrate composition and precipitation rate can influence the processes of channel development. The substrate's texture influences infiltration capacities, which can affect whether precipitation is routed to channels by the surface or subsurface, supporting different processes of channel development. As channels incise through multiple units of glacial sediment, different material properties can introduce complex relationships between precipitation routing and channelization, making it difficult to predict network growth from surficial sediment alone. The prevailing climate sets the frequency and magnitude of precipitation received by a drainage basin, which interacts with the substrate and influences precipitation routing to channels. Coarse-grained, permeable sediments require more frequent or higher magnitude precipitation events to drive overland flow channelization unlike fine-grained, less permeable sediments. If the climate precludes overland flow, then rivers might develop by seepage erosion if relief is sufficient. A lack of both seepage erosion and overland flow can reduce network growth rates, maintaining landscape disconnectivity. While not accounted for in the experiments, climate also controls the density and type of vegetation within a drainage basin. Vegetation can alter precipitation



575 routing to channels by increasing infiltration and constraining erosion by either process, thus impacting drainage network development.

Climate is particularly important in the Central Lowlands, where climate fluctuations including the transition from glacial to interglacial conditions in the late Pleistocene as well as millennial-scale shifts like the Mid-Holocene Warm Period have affected precipitation. The region's drainage networks generally have wide bifurcation angles associated with groundwater-driven channel development supported by the humid climate (Seybold et al., 2017, 2018). However, the dry tundra environment during the last glaciation provided less precipitation to drive channelization but also had less vegetation to resist erosion and increase infiltration. Furthermore, permafrost formation in the soil during glacial periods can inhibit infiltration and drive overland flow (Kasse, 1997). Wetter interglacial periods provide more precipitation to drive channelization, but also increase the amount of vegetation that resists erosion and increases infiltration (Langbein and Schumm, 1958). As the interplay of climate, vegetation, and infiltration change in drainage basins, overland flow or seepage erosion may play a more or less dominant role in channelization through time.

## 6. Conclusions

To gain insight into the processes of channel development in low-gradient landscapes, we conducted small-scale experiments to observe channel development on a low-gradient, internally-drained surface with different rainfall rates, substrate compositions, and a constant rate of base level fall. Several key findings were:

- 590 • Many channels underwent a process transition as they evolved. Channels that initially formed by overland flow transitioned to seepage erosion once channel incision generated enough relief to permit mass wasting via seepage erosion.
  - Landscape variables that mediated infiltration and runoff affected the processes by which channel networks evolved. Overland flow was dominant when conditions favored surface water accumulation, namely, when the substrate had a lower infiltration capacity (i.e., more clay) or when the rainfall rate considerably outpaced infiltration. Seepage erosion was dominant when the substrate was less cohesive and had a higher infiltration capacity (i.e., less clay), which allowed more precipitation to enter the subsurface and reduced the force needed for seepage erosion to occur.
  - 595 • Overall erosional competence of overland flow versus seepage-driven erosion was dependent upon both the areal extent eroding via each process as well as the rate of erosion. For example, overland flow channels eroded greater volumes of sediment due to their extensive channelized area but had smaller incision rates than seepage erosion.
- 600



- In these experiments, overland flow channels had a larger upland CA compared to seepage erosion, allowing overland flow to integrate more NCA as channels eroded headward. Since overland flow was the dominant process throughout most experiments, channels integrated NCA at similar rates under all conditions.

We considered the implications of these findings for drainage networks in the glaciated Central Lowlands where channels have developed in low-gradient topography by integrating NCA through time. The experimental results suggest that the degree of channel incision, glacial sediment texture, and changing climate likely influenced the dominant pathway by which precipitation reached channels. Whether precipitation traveled primarily via the surface or subsurface would favor overland flow or seepage erosion at different points in time and space. If past conditions consistently supported overland flow, then channels may have integrated NCA at a relatively constant rate after an early period of channel initiation. However, post-glacial landscapes include vegetation, topographic features, and complex geology that likely caused the pace of channel development to vary more through time and space than the idealized experiments.

### Data Availability

All data are available through the University of Minnesota Digital Conservancy (Sockness and Gran, 2021, <https://hdl.handle.net/11299/224734>) including all raw DEM data as TIFF files and JPEG images as well as analyzed data in ArcGIS map package files. Data are also linked to the M.S. thesis of Brian Sockness (2020) at <https://hdl.handle.net/11299/213050>.

### Author contribution

BS planned and conducted all experiments and analyses and wrote the manuscript from his M.S. thesis. KG secured funding, advised BS on his M.S. thesis research, and helped with manuscript revisions.

### Competing Interests

The authors declare they have no conflict of interest.

### Acknowledgements

The research was funded by a grant from the U.S. National Science Foundation (EAR-1656969). We appreciate the discussions and assistance from Alison Anders, Pete Moore, Bradley Miller, Cecilia Cullen, Nooreen Meghani, and Joshua McDanel and technical assistance in the laboratory from UMD students Paige Melius, Hannah Schwartz, Elizabeth Boor, and Heidi Krauss.



## References

- Abotalib, A. Z., Sultan, M. and Elkadiri, R.: Groundwater processes in Saharan Africa: Implications for landscape evolution in arid environments, *Earth-Science Rev.*, 156, 108–136, doi:10.1016/j.earscirev.2016.03.004, 2016.
- Abrams, D. M., Lobkovsky, A. E., Petroff, A. P., Straub, K. M., McElroy, B., Mohrig, D. C., Kudrolli, A. and Rothman, D. H.: Growth laws for channel networks incised by groundwater flow, *Nat. Geosci.*, 2(3), 193–196, doi:10.1038/ngeo432, 2009.
- Altin, T. B. and Altin, B. N.: Development and morphometry of drainage network in volcanic terrain, Central Anatolia, Turkey, *Geomorphology*, 125(4), 485–503, doi:10.1016/j.geomorph.2010.09.023, 2011.
- Babault, J., Van Den Driessche, J. and Teixell, A.: Longitudinal to transverse drainage network evolution in the High Atlas (Morocco): The role of tectonics, *Tectonics*, 31(4), 1–15, doi:10.1029/2011TC003015, 2012.
- 635 Berhanu, M., Petroff, A., Devauchelle, O., Kudrolli, A., and Rothman, D. H.: Shape and dynamics of seepage erosion in a horizontal granular bed, *Phys. Rev. E*, 86, 041304, <https://doi.org/10.1103/PhysRevE.86.041304>, 2012.
- Bonnet, S. and Crave, A.: Landscape response to climate change: Insights from experimental modeling and implications for tectonic versus climatic uplift of topography, *Geology*, 31(2), 123–126, doi:10.1130/0091-7613(2003)031<0123:LRTCCI>2.0.CO;2, 2003.
- 640 Brooks, J. R., Mushet, D. M., Vanderhoof, M. K., Leibowitz, S. G., Christensen, J. R., Neff, B. P., Rosenberry, D. O., Rugh, W. D. and Alexander, L. C.: Estimating Wetland Connectivity to Streams in the Prairie Pothole Region: An Isotopic and Remote Sensing Approach, *Water Resour. Res.*, 54(2), 955–977, doi:10.1002/2017WR021016, 2018.
- Castelltort, S. and Simpson, G.: River spacing and drainage network growth in widening mountain ranges, *Basin Res.*, 18, 267–276, doi:10.1111/j.1365-2117.2006.00293.x, 2006.
- 645 Castillo, C. and Gómez, J. A.: A century of gully erosion research: Urgency, complexity and study approaches, *Earth-Science Rev.*, 160, 300–319, doi:10.1016/j.earscirev.2016.07.009, 2016.
- Clayton, L. and Moran, S. R.: Chronology of late wisconsinan glaciation in middle North America, *Quat. Sci. Rev.*, 1, i–vi, doi:10.1016/0277-3791(84)90018-0, 1982.
- Coelho Netto, A. L., Fernandes, N. F. and de Deus, C. E.: Gullying in the southeastern Brazilian Plateau, Bananal, SP, in  
 650 *Sediment Budgets, Proceedings of the Porto Alegre Symposium*, pp. 35–42, IAHS Publication No. 174., 1988.
- Cohen, Y., Devauchelle, O., Seybold, H. F., Yi, R. S., Szymczak, P., and Rothman, D. H.: Path selection in the growth of



- rivers, *Proc Natl Acad Sci USA*, 112, 14132–14137, <https://doi.org/10.1073/pnas.1413883112>, 2015.
- D’Alpaos, A., Lanzoni, S., Marani, M., Fagherazzi, S. and Rinaldo, A.: Tidal network ontogeny: Channel initiation and early development, *J. Geophys. Res. Earth Surf.*, 110(2), 1–14, doi:10.1029/2004JF000182, 2005.
- 655 D’Alpaos, A., Lanzoni, S., Marani, M. and Rinaldo, A.: Landscape evolution in tidal embayments: Modeling the interplay of erosion, sedimentation, and vegetation dynamics, *J. Geophys. Res. Earth Surf.*, 112(1), 1–17, doi:10.1029/2006JF000537, 2007.
- Daag, A. and Van Westen, C. J.: Cartographic modelling of erosion in pyroclastic flow deposits of Mount Pinatubo, Philippines, *ITC J.*, (2), 110–124, 1996.
- 660 Daag, A. S.: Modelling the erosion of the pyroclastic flow deposits and the occurrences of Lahars at Mt. Pinatubo, Philippines, Universiteit Utrecht., 2003.
- Devauchelle, O., Petroff, A. P., Lobkovsky, A. E., and Rothman, D. H.: Longitudinal profile of channels cut by springs, *J. Fluid Mech.*, 667, 38–47, <https://doi.org/10.1017/S0022112010005264>, 2011.
- Devauchelle, O., Petroff, A. P., Seybold, H. F., and Rothman, D. H.: Ramification of stream networks, *Proceedings of the*  
 665 *National Academy of Sciences*, 109, 20832–20836, <https://doi.org/10.1073/pnas.1215218109>, 2012.
- Douglass, J. and Schmeeckle, M.: Analogue modeling of transverse drainage mechanisms, *Geomorphology*, 84(1–2), 22–43, doi:10.1016/j.geomorph.2006.06.004, 2007.
- Douglass, J., Meek, N., Dorn, R. I. and Schmeeckle, M. W.: A criteria-based methodology for determining the mechanism of transverse drainage development, with application to the Southwestern United States, *Bull. Geol. Soc. Am.*, 121(3–4), 586–  
 670 598, doi:10.1130/B26131.1, 2009.
- Dunne, T.: Formation and controls of channel networks, *Prog. Phys. Geogr.*, 4(2), 211–239, doi:10.1177/030913338000400204, 1980.
- Dunne, T.: Hydrology mechanics, and geomorphic implications of erosion by subsurface flow, *Spec. Pap. Geol. Soc. Am.*, 252(January 1988), 1–28, doi:10.1130/SPE252-p1, 1990.
- 675 Dunne, T., Zhang, W. and Aubry, B. F.: Effects of Rainfall, Vegetation, and Microtopography on Infiltration and Runoff, *Water Resour. Res.*, 27(9), 2271–2285, doi:10.1029/91WR01585, 1991.



- Fagherazzi, S., Kirwan, M. L., Mudd, S. M., Guntenspergen, G. R., Temmerman, S., D'Alpaos, A., Van De Koppel, J., Rybczyk, J. M., Reyes, E., Craft, C. and Clough, J.: Numerical models of salt marsh evolution: Ecological, geomorphic, and climatic factors, *Rev. Geophys.*, 50(1), 1–28, doi:10.1029/2011RG000359, 2012.
- 680 Foufoula-Georgiou, E., Takbiri, Z., Czuba, J. A. and Schwenk, J.: The change of nature and the nature of change in agricultural landscapes: Hydrologic regime shifts modulate ecological transitions, *Water Resour. Res.*, 51, 1–23, doi:10.1016/0022-1694(68)90080-2, 2015.
- Garcia, M. and Hérail, G.: Fault-related folding, drainage network evolution and valley incision during the Neogene in the Andean Precordillera of Northern Chile, *Geomorphology*, 65(3–4), 279–300, doi:10.1016/j.geomorph.2004.09.007, 2005.
- 685 Gazetti, E. W.: Autogenic signals in an experimental source-to-sink system, University of Minnesota Duluth. [online] Available from: <https://hdl.handle.net/11299/178910>, 2015.
- Glock, W. S.: The Development of Drainage Systems: A Synoptic View, *Geogr. Rev.*, 21(3), 475–482, doi:10.2307/209434, 1931.
- Gomez, B. and Mullen, V. T.: An experimental study of sapped drainage network development, *Earth Surf. Process. Landforms*, 17(5), 465–476, doi:10.1002/esp.3290170506, 1992.
- 690 Gran, K. B., Belmont, P., Day, S. S., Jennings, C., Johnson, A., Perg, L. and Wilcock, P. R.: Geomorphic evolution of the Le Sueur River, Minnesota, USA, and implications for current sediment loading., 2009.
- Gran, K. B., Finnegan, N., Johnson, A. L., Belmont, P., Wittkop, C. and Rittenour, T.: Landscape evolution, valley excavation, and terrace development following abrupt postglacial base-level fall, *Bull. Geol. Soc. Am.*, 125(11–12), 1851–1864, doi:10.1130/B30772.1, 2013.
- 695 Grimaud, J.-L., Paola, C. and Voller, V.: Experimental migration of knickpoints: influence of style of base-level fall and bed lithology, *Earth Surf. Dyn.*, 4(1), 11–23, doi:10.5194/esurf-4-11-2016, 2016.
- Hasbargen, L. and Paola, C.: Landscape instability in an experimental drainage basin, *Geology*, 28(12), 1,61–67,70, doi:10.1130/0091-7613(2000)28<1067:LIIAED>2.0.CO;2, 2000.
- 700 Hilgendorf, Z., Wells, G., Larson, P. H., Millett, J. and Kohout, M.: From basins to rivers: Understanding the revitalization and significance of top-down drainage integration mechanisms in drainage basin evolution, *Geomorphology*, 352, 107020, doi:10.1016/j.geomorph.2019.107020, 2020.



- Hovius, N., Stark, C. P., Tutton, M. A. and Abbott, L. D.: Landslide-driven drainage network evolution in a pre-steady-state mountain belt: Finisterre Mountains, Papua New Guinea, *Geology*, 26(12), 1071–1074, doi:10.1130/0091-7613(1998)026<1071:LDDNEI>2.3.CO;2, 1998.
- Howard, A. D.: Groundwater sapping experiments and modeling, *Sapping Featur. Color. Plateau a Comp. Planet. Geol. F. Guid.*, 71–83, 1988.
- Howard, A. D. and McLane, C. F.: Erosion of cohesionless sediment by groundwater seepage, *Water Resour. Res.*, 24(10), 1659–1674, doi:10.1029/WR024i010p01659, 1988.
- Huang, J., Wu, P. and Zhao, X.: Effects of rainfall intensity, underlying surface and slope gradient on soil infiltration under simulated rainfall experiments, *Catena*, 104, 93–102, doi:10.1016/j.catena.2012.10.013, 2013.
- Janda, R. J., Meyer, D. F. and Childer, D.: Sedimentation and Geomorphic changes during and following the 1980-1983 eruptions on Mount St. Helens, Washington, *J. Japan Soc. Eros. Control Eng.*, 37(2), 10–21, 1984.
- Kasse, C.: Cold-Climate Aeolian Sand-Sheet Formation in North-Western Europe (c. 14±12.4 ka); a Response to Permafrost Degradation and Increased Aridity, John Wiley & Sons., 1997.
- Kochel, R. C. and Piper, J. F.: Morphology of large valleys on Hawaii: Evidence for groundwater sapping and comparisons with Martian valleys, *J. Geophys. Res.*, 91(B13), E175, doi:10.1029/jb091ib13p0e175, 1986.
- Labbaugh, J. W., Winter, T. C. and Rosenberry, D. O.: Hydrologic Functions of Prairie Wetlan, *Gt. Plains Res.*, 8(1), 17–37 [online] Available from: <https://about.jstor.org/terms> (Accessed 13 May 2021), 1998.
- Lague, D., Crave, A. and Davy, P.: Laboratory experiments simulating the geomorphic response to tectonic uplift, *J. Geophys. Res. Solid Earth*, 108(B1), ETG 3-1-ETG 3-20, doi:10.1029/2002jb001785, 2003.
- Lai, J. and Anders, A. M.: Modeled Postglacial Landscape Evolution at the Southern Margin of the Laurentide Ice Sheet: Hydrological Connection of Uplands Controls the Pace and Style of Fluvial Network Expansion, *J. Geophys. Res. Earth Surf.*, 123(5), 967–984, doi:10.1029/2017JF004509, 2018.
- Laity, J. E. and Malin, M. C.: Sapping processes and the development of theater-headed valley networks on the Colorado Plateau., *Geol. Soc. Am. Bull.*, 96(2), 203–217, doi:10.1130/0016-7606(1985)96<203:SPATDO>2.0.CO;2, 1985.
- Langbein, W. B. and Schumm, S. A.: Yield of sediment in relation to mean annual precipitation, *Eos, Trans. Am. Geophys. Union*, 39(6), 1076–1084, doi:10.1029/TR039i006p01076, 1958.



- Lapotre, M. G. A. and Lamb, M. P.: Substrate controls on valley formation by groundwater on Earth and Mars, *Geology*, 46(6), 531–534, doi:10.1130/G40007.1, 2018.
- Leibowitz, S. G. and Vining, K. C.: Temporal connectivity in a prairie pothole complex, *Wetlands*, 23(1), 13–25, doi:10.1672/0277-5212(2003)023[0013:TCIAPP]2.0.CO;2, 2003.
- Leibowitz, S. G., Mushet, D. M. and Newton, W. E.: Intermittent Surface Water Connectivity: Fill and Spill Vs. Fill and Merge Dynamics, *Wetlands*, 36, 323–342, doi:10.1007/s13157-016-0830-z, 2016.
- Lobkovsky, A. E.: Threshold phenomena in erosion driven by subsurface flow, *J. Geophys. Res.*, 109(F4), 4010, doi:10.1029/2004jf000172, 2004.
- Lusardi, B. A., Gowan, A. S., McDonald, J. M., Marshall, K. J., Meyer, G. N. and Wagner, K. G.: S-23 Geologic Map of Minnesota - Quaternary Geology, St. Paul, Minnesota. [online] Available from: <https://hdl.handle.net/11299/208552>, 2019.
- Maroukian, H., Gaki-Papanastassiou, K., Karymbalis, E., Vouvalidis, K., Pavlopoulos, K., Papanastassiou, D. and Albanakis, K.: Morphotectonic control on drainage network evolution in the Perachora Peninsula, Greece, *Geomorphology*, 102(1), 81–92, doi:10.1016/j.geomorph.2007.07.021, 2008.
- Matsch, C. L.: River Warren, the southern outlet to glacial Lake Agassiz, in *Glacial Lake Agassiz*, edited by J. T. Teller and L. Clayton, pp. 231–244, Geological Society of America Special Paper 26., 1983.
- Micallef, A., Marchis, R., Saadatkhan, N., Pondthai, P., Everett, M. E., Avram, A., Timar-Gabor, A., Cohen, D., Preca Trapani, R., Weymer, B. A. and Wernette, P.: Groundwater erosion of coastal gullies along the Canterbury coast (New Zealand): A rapid and episodic process controlled by rainfall intensity and substrate variability, *Earth Surf. Dyn.*, 9(1), 1–18, doi:10.5194/esurf-9-1-2021, 2021.
- Morbidelli, R., Saltalippi, C., Flammini, A., Cifrodelli, M., Corradini, C. and Govindaraju, R. S.: Infiltration on sloping surfaces: Laboratory experimental evidence and implications for infiltration modeling, *J. Hydrol.*, 523, 79–85, doi:10.1016/j.jhydrol.2015.01.041, 2015.
- Mu, W., Yu, F., Li, C., Xie, Y., Tian, J., Liu, J. and Zhao, N.: Effects of rainfall intensity and slope gradient on runoff and soil moisture content on different growing stages of spring maize, *Water (Switzerland)*, 7(6), 2990–3008, doi:10.3390/w7062990, 2015.
- Nassif, S. H. and Wilson, E. M.: The influence of slope and rain intensity on runoff and infiltration, *Hydrol. Sci. Bull.*, 20(4), 539–553, doi:10.1080/02626667509491586, 1975.



- Neff, B. P. and Rosenberry, D. O.: Groundwater Connectivity of Upland-Embedded Wetlands in the Prairie Pothole Region, Wetlands, 38(1), 51–63, doi:10.1007/s13157-017-0956-7, 2018.
- Onda, Y.: Seepage erosion and its implication to the formation of amphitheatre valley heads: A case study at Obara, Japan, Earth Surf. Process. Landforms, 19, 627–640, 1994.
- 760 Ouchi, S.: Effects of uplift on the development of experimental erosion landform generated by artificial rainfall, Geomorphology, 127(1–2), 88–98, doi:10.1016/j.geomorph.2010.12.009, 2011.
- Parker, R. S.: Experimental study of drainage basin evolution and its hydrologic implications, Colo State Univ (Fort Collins) Hydrol Pap, (90) [online] Available from: <https://apps.dtic.mil/sti/citations/ADA051839> (Accessed 13 May 2021), 1977.
- Pelletier, J. D.: Drainage basin evolution in the Rainfall Erosion Facility: Dependence on initial conditions, Geomorphology, 765 53(1–2), 183–196, doi:10.1016/S0169-555X(02)00353-7, 2003.
- Petroff, A. P., Devauchelle, O., Abrams, D. M., Lobkovsky, A. E., Kudrolli, A., and Rothman, D. H.: Geometry of Valley Growth, J. Fluid Mech., 673, 245–254, <https://doi.org/10.1017/S002211201100053X>, 2011.
- Petroff, A. P., Devauchelle, O., Seybold, H., and Rothman, D. H.: Bifurcation dynamics of natural drainage networks, Phil. Trans. R. Soc. A., 371, 20120365, <https://doi.org/10.1098/rsta.2012.0365>, 2013.
- 770 Phillips, L. F. and Schumm, S. A.: Effect of regional slope on drainage networks., Geology, 15(9), 813–816, doi:10.1130/0091-7613(1987)15<813:EORSOD>2.0.CO;2, 1987.
- Pillans, B.: Drainage initiation by subsurface flow in South Taranaki, New Zealand., Geology, 13(4), 262–265, doi:10.1130/0091-7613(1985)13<262:DIBSFI>2.0.CO;2, 1985.
- Poesen, J., Nachtergaele, J., Verstraeten, G. and Valentin, C.: Gully erosion and environmental change: Importance and 775 research needs, Catena, 50(2–4), 91–133, doi:10.1016/S0341-8162(02)00143-1, 2003.
- Rosenberry, D. O. and Winter, T. C.: Dynamics of water-table fluctuations in an upland between two prairie-pothole wetlands in North Dakota, J. Hydrol., 191(1–4), 266–289, doi:10.1016/S0022-1694(96)03050-8, 1997.
- Ruhe, R. V.: Topographic discontinuities of the Des Moines Lob, Am. J. Sci., 1, 46–56, 1952.
- Schottler, S. P., Ulrich, J., Belmont, P., Moore, R., Lauer, J. W., Engstrom, D. R. and Almendinger, J. E.: Twentieth century 780 agricultural drainage creates more erosive rivers, Hydrol. Process., 28(4), 1951–1961, doi:10.1002/hyp.9738, 2014.



- Schumm, S. A.: Evolution and Response of the Fluvial System, Sedimentologic Implications, 1981.
- Schumm, S. A. and Lichty, R. W.: Time, space, and causality in geomorphology, *Am. J. Sci.*, 263(2), 110–119, doi:10.2475/ajs.263.2.110, 1965.
- Schumm, S. A. and Phillips, L.: Composite channels of the Canterbury Plain, New Zealand: a Martian analog?, *Geology*, 14(4), 326–329, doi:10.1130/0091-7613(1986)14<326:CCOTCP>2.0.CO;2, 1986.
- Schumm, S. A., Boyd, K. F., Wolff, C. G. and Spitz, W. J.: A ground-water sapping landscape in the Florida Panhandle, *Geomorphology*, 12(4), 281–297, doi:10.1016/0169-555X(95)00011-S, 1995.
- Seybold, H., Rothman, D. H., and Kirchner, J. W.: Climate’s watermark in the geometry of stream networks, *Geophys. Res. Lett.*, 44, 2272–2280, <https://doi.org/10.1002/2016GL072089>, 2017.
- Seybold, H. J., Kite, E., and Kirchner, J. W.: Branching geometry of valley networks on Mars and Earth and its implications for early Martian climate, *Sci. Adv.*, 4, eaar6692, <https://doi.org/10.1126/sciadv.aar6692>, 2018.
- Shaw, D. A., Vanderkamp, G., Conly, F. M., Pietroniro, A. and Martz, L.: The Fill-Spill Hydrology of Prairie Wetland Complexes during Drought and Deluge, *Hydrol. Process.*, 26(20), 3147–3156, doi:10.1002/hyp.8390, 2012.
- Simon, A.: Channel and drainage-basin response of the Toutle River system in the aftermath of the 1980 eruption of Mount St. Helens, Washington, Open-file Rep., (96–633), x, 130 p., 1999.
- Singh, A., Reinhardt, L. and Foufoula-Georgiou, E.: Landscape reorganization under changing climatic forcing: Results from an experimental landscape, *Water Resour. Res.*, 51(6), 4320–4337, doi:10.1002/2015WR017161, 2015.
- Sockness, B.: An Experimental Study of Drainage Network Development by Surface and Subsurface Flow in Low-Gradient Landscapes. Retrieved from the University of Minnesota Digital Conservancy, <https://hdl.handle.net/11299/21305>: 2020.
- Sockness, B., and Gran, K.B.: An experimental study of drainage network development by surface and subsurface flow in low-gradient landscapes raster databases. Retrieved from the Data Repository for the University of Minnesota, <https://hdl.handle.net/11299/224734>, 2021.
- Stichling, W. and Blackwell, S. R.: Drainage area as a hydrologic factor on the glaciated Canadian prairies, *IUGG Proc.*, 365–367, 1957.
- Sweeney, K. E., Roering, J. J. and Ellis, C.: Experimental evidence for hillslope control of landscape scale, *Science* (80-. ),



- 349(6243), 51–53, doi:10.1126/science.aab0017, 2015.
- Thompson, S. E., Harman, C. J., Heine, P. and Katul, G. G.: Vegetation-infiltration relationships across climatic and soil type gradients, *J. Geophys. Res. Biogeosciences*, 115(G2), n/a-n/a, doi:10.1029/2009jg001134, 2010.
- Tiner, R. W.: Geographically isolated wetlands of the United States, *Wetlands*, 23(3), 494–516, doi:10.1672/0277-5212(2003)023[0494:GIWOTU]2.0.CO;2, 2003.
- 810 Turowski, J. M., Lague, D., Crave, A. and Hovius, N.: Experimental channel response to tectonic uplift, *J. Geophys. Res. Earth Surf.*, 111(3), doi:10.1029/2005JF000306, 2006.
- Uchupi, E. and Oldale, R. N.: Spring sapping origin of the enigmatic relict valleys of Cape Cod and Martha’s Vineyard and Nantucket Islands, Massachusetts, *Geomorphology*, 9(2), 83–95, doi:10.1016/0169-555X(94)90068-X, 1994.
- 815 Valentin, C., Poesen, J. and Li, Y.: Gully erosion: Impacts, factors and control, in *Catena*, vol. 63, pp. 132–153, Elsevier., 2005.
- Whipple, K. X., DiBiase, R. A., Ouimet, W. B. and Forte, A. M.: Preservation or piracy: Diagnosing low-relief, high-elevation surface formation mechanisms, *Geology*, 45(1), 91–94, doi:10.1130/G38490.1, 2017.
- Winter, T. C.: *Relation of streams, lakes, and wetlands to groundwater flow systems*, Springer-Verlag., 1999.
- 820 Winterberg, S. and Willett, S. D.: Greater Alpine river network evolution, interpretations based on novel drainage analysis, *Swiss J. Geosci.*, 112(1), 3–22, doi:10.1007/s00015-018-0332-5, 2019.